Applied Physics B (2022) 128:49
https://doi.org/10.1007/s00340-021-07729-z

Applied Physics B
Lasers and Optics

Roadmap on chaos-inspired imaging technologies (CI^2-Tech)

Joseph Rosen[1] · Hilton B. de Aguiar[2] · Vijayakumar Anand[3,16] · YoonSeok Baek[4] · Sylvain Gigan[2] · Ryoichi Horisaki[5] · Hervé Hugonnet[4] · Saulius Juodkazis[3,6] · KyeoReh Lee[4] · Haowen Liang[7] · Yikun Liu[7] · Stephan Ludwig[8] · Wolfgang Osten[8] · YongKeun Park[4,9] · Giancarlo Pedrini[8] · Tushar Sarkar[10] · Johannes Schindler[8] · Alok Kumar Singh[8] · Rakesh Kumar Singh[9] · Guohai Situ[11,12,13] · Mitsuo Takeda[14] · Xiangsheng Xie[7,15] · Wanqin Yang[11,12] · Jianying Zhou[7]

Received: 1 September 2021 / Accepted: 1 December 2021 / Published online: 14 February 2022

Abstract

In recent years, rapid developments in imaging concepts and computational methods have given rise to a new generation of imaging technologies based on chaos. These chaos-inspired imaging technologies (CI^2-Tech) consist of two directions: non-invasive and invasive. Non-invasive imaging, a much older research direction with a goal of imaging through scattering layers, has reached faster, smarter, and sharper imaging capabilities in recent years. The invasive imaging direction is based on exploiting the chaos to achieve imaging characteristics and increase dimensionalities beyond the limits of conventional imagers. In this roadmap, the current and future challenges in invasive and non-invasive imaging technologies are presented.

✉ Vijayakumar Anand
vijayakumar.anand@ut.ee

[1] School of Electrical and Computer Engineering, Ben-Gurion University of the Negev, PO Box 653, 8410501 Beer-Sheva, Israel

[2] Laboratoire Kastler Brossel, ENS-Université PSL, CNRS, Sorbonne Université, Collège de France, 24 rue Lhomond, 75005 Paris, France

[3] Optical Sciences Centre and ARC Training Centre in Surface Engineering for Advanced Materials (SEAM), School of Science, Swinburne University of Technology, Hawthorn, VIC 3122, Australia

[4] Department of Physics, Korea Advanced Institutes of Science and Technology, Daejeon 34141, South Korea

[5] Graduate School of Information Science and Technology, The University of Tokyo, 7-3-1 Hongo, Bunkyo-ku, Tokyo 113-8656, Japan

[6] Tokyo Tech World Research Hub Initiative (WRHI), School of Materials and Chemical Technology, Tokyo Institute of Technology, 2-12-1, Ookayama, Meguro-ku, Tokyo 152-8550, Japan

[7] School of Physics, State Key Laboratory of Optoelectronic Materials and Technology, Southern Marine Science and Engineering Guangdong Laboratory (Zhuhai), Sun Yat-sen University, Guangzhou 510275, China

[8] Institut fuer Technische Optik, Universitaet Stuttgart, Pfaffenwaldring 9, 70569 Stuttgart, Germany

[9] Tomocube, Inc., Daejeon 34051, Republic of Korea

[10] Department of Physics, Indian Institute of Technology (BHU), Varanasi 221005, India

[11] Shanghai Institute of Optics and Fine Mechanics, Chinese Academy of Sciences, Shanghai 201800, China

[12] Center of Materials Science and Optoelectronics Engineering, University of Chinese Academy of Sciences, Beijing 100049, China

[13] Hangzhou Institute for Advanced Study, University of Chinese Academy of Sciences, Hangzhou 310024, China

[14] Center for Optical Research and Education, Utsunomiya University, Utsunomiya 321-8585, Japan

[15] Department of Physics, College of Science, Shantou University, Shantou 515063, Guangdong, China

[16] Present Address: Institute of Physics, University of Tartu, Tartu 50411, Estonia

1 Introduction (Vijayakumar Anand and Joseph Rosen)

Chaos has been considered an undesirable phenomenon in almost all areas of research except the field of chaos research. In everyday life, we often encounter chaos in the form of fog, which distorts the information of the object coming to the sensor. In imaging technologies, there are numerous techniques developed to suppress different forms of chaos and render a noise-free image by both real time and post-processing of the recorded image information [1–3]. While the above scenario is evident, during the past decade, many prominent imaging scientists have been leading a radically different research direction of introducing chaos into imaging systems and exploiting the behavior to perform advanced imaging [4–12]. As a matter of fact, the above researchers have set a new research direction in imaging, which has been followed by many researchers across the world, resulting in flooding of leading research journals by articles on chaos-inspired imaging technologies (CI^2-Tech). We believe that the time is right to write a roadmap on this rapidly evolving topic.

In general, CI^2-Techs can be classified into invasive and non-invasive. The former requires additional information in the form of the pre-recorded point spread functions (PSFs) or phase image of the scatterer to reconstruct the object information [13–15], while the latter can reconstruct the object information by processing only the scattered intensity distributions obtained for an object [16–18]. The invasive approaches can offer capabilities to image simultaneously in multiple dimensions such as depth and wavelength, where images can be captured in a single shot of a monochrome camera, with high resolution and wide field of view. One main drawback is the invasive nature, where the PSF library needs to be recorded at all depths or wavelengths, and the recording must be repeated every time the optical setup is changed. The non-invasive approaches require a phase-retrieval algorithm to reconstruct the object information, which may preclude their applications to real-time imaging. In addition, the quality of images obtained, and the field of view are limited. However, in recent years due to the rapid developments in both invasive and non-invasive approaches, most of the above problems have been minimized to a great extent, and many new capabilities have been demonstrated.

The CI^2-Techs are good examples of how computational optical methods function, where cumbersome optical configurations, two-wave interference, and vibration isolation can be successfully replaced by signal processing and computational tools creating simpler, low-cost imaging technologies with advanced capabilities. Even though CI^2-Techs have been investigated in the past as early as 1968 [19], the rationale for the current boom in research on this topic, especially during the last decade, must be attributed to the developments in computational optics and new electrooptical devices. Worth noting, the development of the widely used Fienup-type phase-retrieval algorithms was in 1982, while the demonstration of non-invasive imaging occurred in 2012 [20]. This time gap is fascinating as to how significant the difference in impact can be depending on at what point in time an idea was invented.

Some notable inventions in CI^2-Tech are as follows: the interferenceless coded aperture correlation holography (I-COACH) developed by the research group of Rosen in 2017 led to numerous studies on this topic, including a single-shot adaptive non-linear reconstruction method [21]. Two major inventions were reported by the research group of Osten and Takeda in invasive as well as non-invasive approaches [6, 22, 23]. A scatter-plate microscope was used with a resolution of 4 μm in the invasive mode. The non-invasive approach was built on two ideas: namely, the relative phase information between object and reference is preserved during scattering and statistical averaging. Other notable studies on invasive imaging were reported by Wagadarikar et al. [15] and Antipa et al. [13] on spectral and spatial imaging, respectively. Recently, the spectral imaging was demonstrated over a large field of view by the research group of Zhou [9]. The same group successfully applied scaling factors to the recorded point spread functions (PSFs) to image at various depths [24]. The approach substantially reduced the training duration of invasive approaches. In this direction, the depth–wavelength reciprocity was identified by the research group of Juodkazis, which led to seeing color from the depth and vice versa and demonstrated five-dimensional imaging from a single camera shot and highly reduced pre-training [12]. This approach avoided the need for light sources with different colors for the pre-training.

Some notable non-invasive approaches were developed by Bertolotti et al. [16] and Katz et al. [17]. A fundamental study on the control of light propagation through scattering media was done by the group of Gigan [25, 26]. A non-invasive three-dimensional (3D) imaging method by exploiting the scaling factors in phase retrieval was developed by Horisaki et al. [18]. Novel deep learning techniques have been developed by the group of Situ for almost all imaging concepts: holographic imaging [10], imaging through scattering media [27], and computational ghost imaging [28]. A learning-based approach was proposed by Ando et al. by studying the inverse function of the scattering process [29]. Another interesting direction of partially coherent light-based quantitative phase imaging was demonstrated by Lee and Park [5]. A radical approach on correlation holography based on van Cittert–Zernike theorem and the Hanbury Brown–Twiss (HBT) has been proposed recently by the research group of Singh for imaging through scattering layers [11]. This method uses an interferometric approach to record the complex coherence function and retrieves the

object information from the second-order correlation. In this roadmap, some of the major developments in CI^2-Tech and the future perspectives are discussed.

2 Interferenceless coded aperture correlation holography (Joseph Rosen)

2.1 Status

I-COACH was proposed in 2017 [8] as a simpler version of the incoherent holographic method termed coded aperture correlation holography (COACH) [30]. Both COACH and I-COACH spatially modify incoherent light by coded phase masks (CPMs), but unlike COACH, I-COACH operates without two-beam interference. I-COACH is a three-dimensional (3D) incoherent imaging technique in which the image is reconstructed by two-dimensional cross-correlation between the object hologram and a library of point spread holograms (PSHs) acquired in advance in the calibration mode of the system. The light beams from the calibrating points and from the object are modulated by the same chaotic CPMs and recorded by a digital camera after propagating in the free space. A simpler system like I-COACH without two-beam interference can yield a similar result to COACH, because the intensity response of I-COACH to an input point is highly sensitive to the axial location of this point. In formal wording, this sensitivity means that the cross-correlation between two intensity responses to points located at two different axial locations is much smaller than the autocorrelation of each response. Therefore, with the intensity distributions recorded by the camera, the entire object points can be reconstructed in the 3D image space by operations of cross-correlation described next in more detail.

The initial design [8] has evolved into various systems with different architectures and algorithms, each of which has its own advantages and weaknesses. The basic scheme of I-COACH is shown in Fig. 1, in which the same physical system is schematically described in two modes of operation. The upper scheme illustrates the calibration mode, in which the system accumulates a library of PSHs recorded for a source point located at various axial locations. Once the library is complete, the same physical system operates in the imaging mode shown in the lower part of Fig. 1. The single source point is replaced by an incoherently illuminated 3D object, and its intensity response is cross-correlated with each member of the library. The result of the 2D cross-correlations is the desired reconstructed 3D image. This scheme is generic and has been the basis for most developments of I-COACH evolved since 2017, which are briefly described next.

Any technology of recording images is aimed to be as fast as possible with minimum camera shots. While the initial version of I-COACH [8] has been demonstrated with three independent CPMs, and three camera shots, in [31], the number of CPMs and shots were reduced to two. Another interesting feature of [31] is the use of a system without refractive lenses achieved by a different

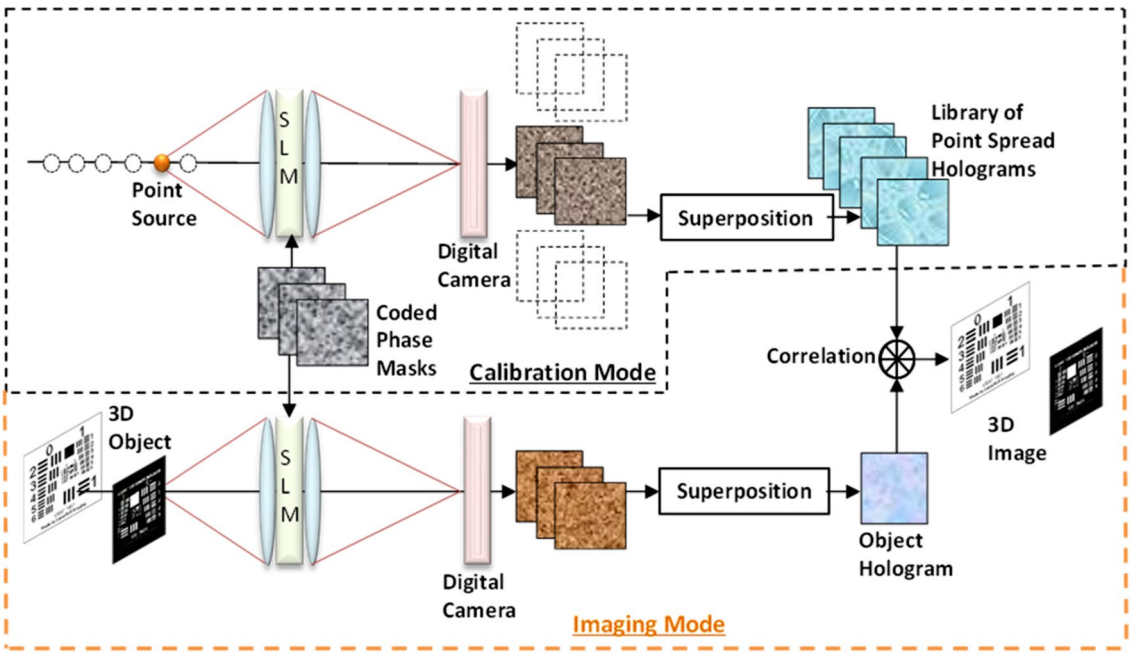

Fig. 1 Schematic of I-COACH for recording library of PSHs (top) and 3D imaging (bottom)

method of synthesizing the CPMs. A single-camera shot was achieved in [32] by multiplexing two CPMs in space instead of time as before [8, 31]. The field of view (FoV) has been extended in the I-COACH demonstrated in [33] by calibrating the system with extended (beyond the conventional FoV) PSHs. The digital reconstruction process was modified in [21] by replacing the linear cross-correlation with nonlinear cross-correlation optimized to yield correlation peaks with a minimum entropy. A modified nonlinear cross-correlation with a different optimization cost function was applied in [35]. Part of the image noise in the above-mentioned versions [8, 31–34] came from a low-intensity level of the PSH on the camera plane. This problem was fixed in [36] by enforcing a PSH in the shape of sparse dots of light distributed randomly inside a limited area. A different solution to the same problem was proposed in [37], where the proposed PSH was in the shape of a ring. The calibration process in the upper part of Fig. 1 was replaced by a digital method of synthesizing a library of PSHs in the computer [38]. Other modifications of I-COACH are related to specific applications and they are summarized in the next subsection.

2.2 Applications

Lateral resolution can be considered one of the holy grails of optical imaging. Improving the lateral resolution by I-COACH has been treated in [39–41] by different approaches. In general, the lateral and axial resolutions of I-COACH are equivalent to those of conventional direct imaging systems with the same numerical aperture. The techniques proposed in [39–41] improve the imaging resolution beyond the diffraction limit imposed by the limited numerical aperture of optical systems. In one of these systems [41] shown in Fig. 2a, a CPM displayed on a spatial light modulator (SLM) is introduced between the object and the input aperture of an ordinary lens-based imaging system. Consequently, the effective numerical aperture is increased beyond the inherent numerical aperture of the imaging system. Unlike conventional systems, in the proposed method, the image of the object is not directly obtained on the camera, but it is based on the I-COACH principles, including a one-time calibration. Following the calibration, the system is ready for imaging an arbitrary number of objects. In [41], the super-resolved image of the object is reconstructed by a nonlinear cross-correlation between the PSH and the object hologram. The effective numerical aperture and the new resolution limit can be tuned by changing the scattering degree of the CPM. An example of the I-COACH image is shown in Fig. 2b in comparison to a direct image obtained from the system of Fig. 2a but without the SLM.

Another application of I-COACH is the partial aperture imaging system (PAIS) [42–44], in which the traditional disk-shaped aperture is replaced by an annular CPM aperture [42, 43] or by several relatively small CPMs distributed on the perimeter of the much larger circle [44]. The lateral resolution of PAIS is the same as direct imaging with the disk-shaped aperture. However, the advantages of PAIS can be saving weight in space-based telescopes [42, 44] or using the free area of the aperture for other applications rather than imaging [43]. I-COACH for recording digital holograms with coherent light but without two-beam interference was demonstrated in [45]. I-COACH can work with coherent light as long as the PSH is an ensemble of sparse dots where the distance between any two dots is larger than the object size. Non-invasive imaging through scattering layers can be more efficient when the I-COACH system is integrated with an iterative method of image retrieval, as is demonstrated in [46]. Depth-of-field (DoF) engineering is another application that has been demonstrated by I-COACH [47]. DoF

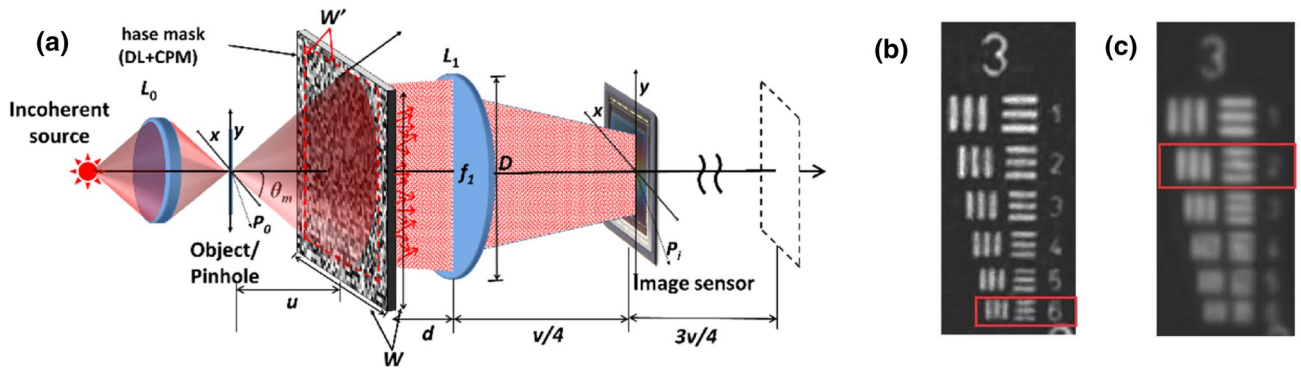

Fig. 2 **a** Optical scheme of the resolution enhancement technique with I-COACH. Broken black lines indicate the image plane of direct imaging. Reconstructed images of **b** I-COACH and **c** direct imaging. Adapted from [41]

engineering means that a system can have one extended DoF, several DoFs at separated intervals in the imaging space, and the separated DoFs can be shifted relative to each other. Practically, these features mean that images can be in focus at certain user-controlled locations in the imaging space. As a final application, we mention here the system of the quasi-random lens as an example of a system like I-COACH, but in which the CPM is implemented as a single constant diffractive element [48]. With certain spatial filters, this system achieved white-light imaging, although the quasi-random lens is a diffractive, highly dispersive element.

2.3 Conclusion and future perspectives

I-COACH is a concept that extends the resources available for imaging. The real-valued aperture function of the direct imaging is replaced with the complex-valued aperture function of I-COACH. Moreover, the I-COACH aperture can be modified over time. Finally, an additional stage of digital processing is integrated with the optical system. These additional resources add to I-COACH capabilities which can add new features to the imaging systems. Although I-COACH is a simpler version of COACH and hence is preferred for most of the 3D imaging tasks, there are several known special applications that COACH, or two-beam interference, is needed. Incoherent synthetic aperture imagers [49, 50] are typical examples for systems that two-beam interference is essential for their operations. However, other applications can be implemented successfully by I-COACH; some of them are presented herein others might be proposed in the future.

3 Coded aperture imaging with synthetic point spread functions (Joseph Rosen, Vijayakumar Anand, and Saulius Juodkazis)

3.1 Status

The preliminary PSH training required in coded aperture imaging (CAI) is cumbersome and must be repeated every time the optical setup is modified. For a single plane, the training procedure is like that of a direct imaging system. However, for multiple planes (p) and for different wavelengths (q) the training is exhaustive involving $p \times q$ measurements. Furthermore, the requirement of the optical sources is enormous, requiring either sources for all visible wavelengths or a wavelength-tunable light source [12–14, 51]. Synthesis of PSHs from one or few recordings was proposed [12, 24, 38] to minimize the number of recorded spatio-spectral PSHs. In the case of thin scatterers, a linear region in object space exists where the intensity distribution of the scattered field at different distances are only scaled versions of one of the recordings. This scaling property has been utilized to reduce the number of measurements of PSHs. Furthermore, the reconstruction of CAI methods can be carried out only at the locations of the pinholes, which are not continuous as it is done with other holography methods such as FINCH. In FINCH, the reconstruction function is a quadratic phase mask whose focal length can be tuned continuously to find the best reconstruction. By utilizing the scaling factor in CAI, continuous tuning of distance can be achieved.

The optical configuration of lensless, interferenceless coded aperture correlation holography (LI-COACH) is

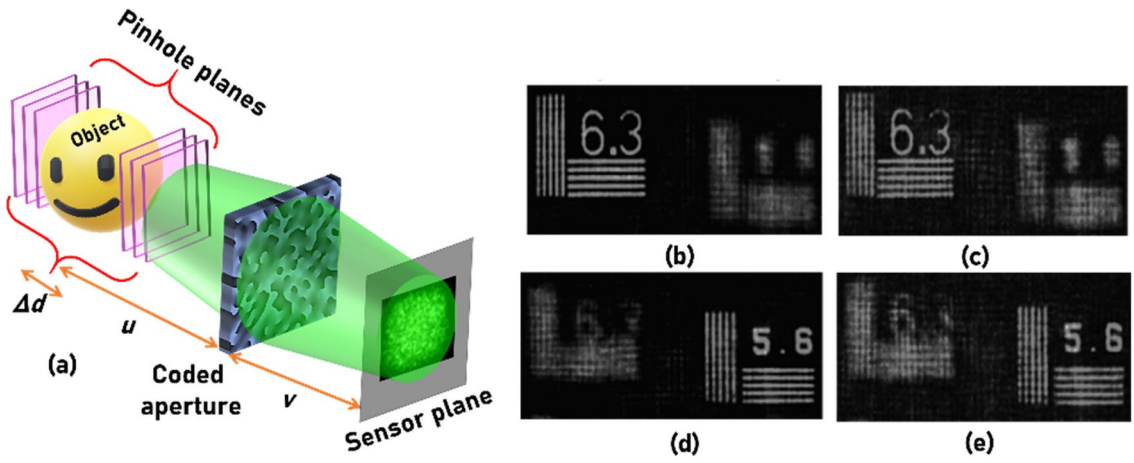

Fig. 3 **a** Optical configuration of lensless, interferenceless coded aperture correlation holography (LI-COACH). Reconstruction results of plane—1 with **b** recorded PSH and **c** synthetic PSH. Reconstruction results of plane—2 with **d** recorded PSH and **e** synthetic PSH (adapted from [38])

shown in Fig. 3a. Two National Bureau of Standards (NBS) objects—6.3 lp/mm and 5.6 lp/mm were mounted in two optical channels at two planes separated by 20 mm. The first object was at $u = 26$ cm from the coded aperture, and the sensor was at $v = 26$ cm from the coded aperture. The reconstruction results of the first NBS object 6.3 lp/mm using recorded PSH and synthetic PSH are shown in Fig. 3b, c, respectively. The reconstruction results of the second NBS object 5.6 lp/mm using recorded PSH and synthetic PSH are shown in Fig. 3d, e, respectively. By comparing the results, it is seen that synthetic PSH was able to reconstruct the complete information with some additional noise components. However, after $d > 25$ mm, the reconstruction results gradually declined, as shown in [24]. Nevertheless, this approach can reduce the number of PSH recordings by at least one order of magnitude in many cases.

The second challenge is the need for a tunable light source. In the quadratic phase function given as $Q(1/z) = \exp[j\pi(x^2 + y^2)/(\lambda z)]$, the denominator term λz is an interesting formation. It means that within the region of parabolic approximation, regardless if λ or z increases, the phase change is the same if the factor of change is the same for both λ and z. So, it is possible to synthesize a phase for a different wavelength by changing depth and vice versa. This condition is called depth–wavelength reciprocity. In [12], the PSH of a different wavelength λ_2 was recorded using λ_1 by changing u and v by a factor of λ_2/λ_1. This is a useful relationship. When the spatio-spectral PSH library was recorded and correlated with one of the elements of the library, then only for the autocorrelation a sharp peak is obtained, and the value decreases when the point is moved away from the reference in space and spectrum. Using the depth–wavelength reciprocity, it is possible to have the cross-correlation values equal to the autocorrelation values. In the optical configuration, as shown in Fig. 3a, the recurrence of the peak is possible only when both u and v are changed by the same factor. The plot of the correlation values when only u was changed, and v was constant, and when both u and v were changed by the same factor are shown in Fig. 4a, b, respectively. The reconstruction result of an NBS object 8.0 recorded by green wavelength and reconstructed by PSH of green wavelength is shown in Fig. 4c. The reconstruction result of the same object using the PSH of red wavelength but with u and v values changed by the factor of ratio between the two wavelengths is shown in Fig. 4d. Comparing Fig. 4c, d, the application of depth–wavelength reciprocity is evident. In some studies, the PSHs were recorded for two extreme wavelengths, and using a linear fit, the PSHs for other wavelengths were synthesized by scaling the recorded PSHs by the factors in the fitted data [52].

3.2 Conclusions and future perspectives

The major problems associated with CAI on spatio-spectral pre-training have been significantly reduced by exploiting the spatio-spectral scaling factors in a linear range of operation within the paraxial region. Consequently, CAI can be operated to image up to five dimensions along with three-dimensional space, spectrum, and time with lowest calibration requirements as a lens-based imaging system. The scaling property and depth-wavelength reciprocity can be utilized smartly to perform advanced imaging for many applications. We believe that the above studies will be valuable when developing CAI-based instruments and products. In some of our studies,

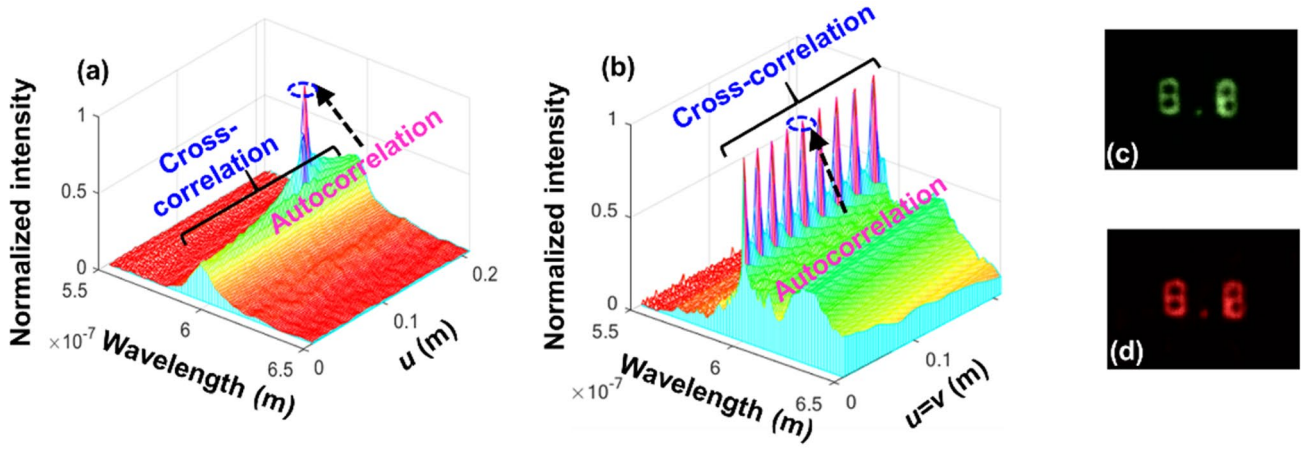

Fig. 4 **a** Plot of correlation values in spatio-spectral space when u was varied, but v was constant **b** when u and v were varied simultaneously by the same factor. Reconstruction results of PSH recorded with **c** green wavelength and **d** red wavelength but by changing u and v by the ratio of wavelengths

we found that the depth–wavelength reciprocity, which is a boon, can also be a bane when recording a multispectral event occurring in confined areas by a monochrome camera. It was difficult to decouple spatial and spectral effects as the same change can be produced by either a change in wavelength or depth. One possible research direction which will remove the need for recording PSH in CAI systems is to synthesize the PSHs directly from the known phase or amplitude function of the coded aperture and the optical configuration of the imaging system.

4 Optical imaging through long-range turbid media (Xiangsheng Xie, Yikun Liu, Haowen Liang, Jianying Zhou)

4.1 Status

Optical imaging through turbid medium has a long history of research, with milk, foam, and ground glass as typical media. Widespread applications for optical imaging through atmosphere or underwater have prompted broad interests in this area. Recent desktop experiment results necessitate to re-examine the progress in the field and to extend the capability of optical imaging in the long-range turbid media.

Long-range optical imaging in turbid media is primarily dealing with atmosphere or underwater. The atmosphere of Earth is composed of a variety of gas molecules and aerosols. These molecules and aerosols have certain absorption and scattering for visible light. The absorption is mainly resulted by water vapor, carbon dioxide, methane, and ozone. The scattering is primary caused by atmospheric aerosol, which has complex chemical composition, different particle size and shape. From a static point of view, the influence of atmosphere on light propagation comes from the refractive index variation, which depends on the meteorological parameters such as air pressure, temperature, and humidity. As shown in Fig. 5, when the atmospheric refractive index fluctuates or varies randomly in time and space, there is atmospheric turbulence. In clean weather with less scattering and with high visibility, the light coming from a long-distance object experiences turbulence and leads to a flickering or warping image, i.e., twinkle stars. In turbid atmosphere, most of the object light is reflected, refracted, scattered, and cannot reach the imaging plane. Part of the remaining light reaches the imaging plane but deviates from the imaging position or angle, resulting in blurred images. Ambient scattering light including scattered sunlight, other luminous object light, thermal light, etc., is added to the image sensor and further reduces the image contrast.

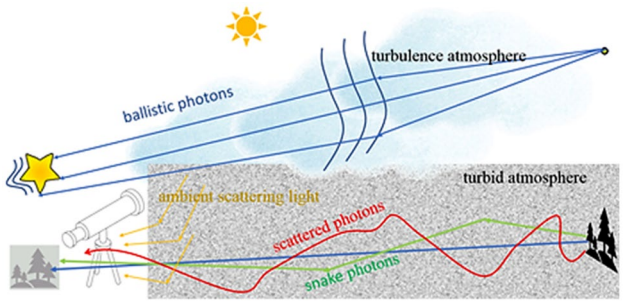

Fig. 5 Schematic of long-range imaging through turbid or turbulent atmosphere

For the case of underwater optical imaging, optical illumination and imaging detection are employed. Although the absorption and scattering mechanism are somewhat different, the same challenges to discriminate the signal from the background remains. Optical imaging under natural sunlight is often employed in the atmosphere while active illumination is commonly adopted for underwater.

The common methods used for image recovery from the hazy atmosphere are digital image processings (DSPs), e.g., fog removal, image dehazing, artificial intelligence optimization and defogging algorithms. New techniques exploit the physics of the scattering problem and discriminate between different types of photon trajectories, including ballistic photons, snake photons and scattered photons. Since the ballistic photons and the snake photons are not strongly scattered, they retain the information of the objects and travel faster than the scattered photons. Time-gated method [53] uses a pulsed laser system and a synchronized high-speed gated camera to select the ballistic photons such as snake like photons for temporal resolution imaging. Polarizing filter method has been proved to be effective for underwater imaging in the backscattering removal and becomes a popular method for underwater imaging by distinguishing the directly reflected ballistic photons from the target. Imaging beyond the ballistic limit is possible by interpreting the scattered light instead of rejecting it. Wavefront-shaping [54] techniques have been employed to compensate the phase of light through highly scattering complex media and even produce super-resolution images of the objects placed beyond opaque screens. Speckle patterns and their correlations have been demonstrated to be effective for image recovery. This speckle correlation method [16] is thought to be a promising solution because it does not need coherent light sources, expensive wavefront modulators, complicated interference setups, nor a time-consuming calibration. The deconvolution approach [9] can reconstruct the image of the object from its speckle and the point spread function (PSF) of the scattering system in real time. By harnessing the spatial, spectral properties of the PSF of a scattering system, large field of view (FOV) beyond the limit of the optical memory effect (OME), extended depth of field (DOF) for 3D imaging, color image reconstruction can be realized in real time [9].

It is obviously that a point source, named as guidestar, within the random medium is one of the most useful things enabled by deconvolution or wavefront shaping methods. The guiding stars first appeared in astronomical observation using adaptive optics which allows the theoretical limit of angular resolution from a large telescope, despite the presence of turbulence. A guidestar is now redefined as any mechanism that produces an effective source (virtual or real) of sufficiently coherent radiation inside a medium. An actual internal source, such as an emitting molecule, an optical nonlinearity, or a modulation of the local material parameters produced by additional fields, e.g., ultrasound waves, could be used as a guidestar. The adaptive optics is still the most efficient method to drastically improve the sharpness of the focus and the resolution in astronomy. However, it typically uses 10–100 degrees of freedom corresponding to the number of pixels of the phase modulator and can only correct the aberrations with a weak scatter. Wavefront shaping technique uses spatial light modulator (SLM) up to millions of pixels, i.e., liquid crystal SLM, digital micro-mirror devices or digital phase conjugation mirror. It has larger degrees of freedom to control the scattered light through more strongly scattering centers and multiple scatters, but still be applied only in short-range turbid space, e.g., biological tissues. For long-range turbid, the extremely weak contrast caused by dispersion and loss of light is the major limiting factors. Another more important limitation is the atmospheric dynamics, the measurement plus the control of millions of pixels of the SLM has to be faster than the fluctuating speckles.

A new method using the Fourier-domain shower-curtain effect [55] can overcome the dynamics of both turbid media and the object for imaging. It has been developed into a non-invasive coaxial reflective configuration. But for long-range imaging, a free propagation distance is needed to realize the conversion from object plane to Fourier-domain and a thin screen to display the speckle. Even more, all these speckle-based methods are challenging to implement through a mass of aerosols because the speckle decorrelation is sensitive to moving scatters especially when the transport optical depth t is larger than 2. Alternatively, it is possible to use incoherent methods, for example, diffuse optical imaging (DOI), to estimate the locations and the shapes of objects in tissue for $t < 100$. A new model [56] has been proposed to extend the DOI to the moderately scattering regime in fog. By detecting the time of flight (TOF) information of the photons reflected by the hidden object, non-line of sight (NLOS) imaging can track and image a hidden object at long ranges up to 1.43 km [57]. When going toward longer ranges, the atmospheric turbulence will be the major factor to disable the NLOS technique unless advanced devices such as shorter pulse lasers, higher efficiency detectors are used to select the ballistic photons.

Optical imaging in long-range turbid space is always a scientific and technological challenge. The current methods include PSF estimation, DSP, computational, etc., can only recover within the visibility range at a limited distance. The averaging method is commonly used in the ballistic photon-based techniques because the speckle can be averaged as uniform background. On the other hand, averaging gives rise to other problems such as blurring. Mitigating the deleterious effects of scattering and turbulence in atmosphere are equally important. New techniques exploit the physics of the scattering problem and have been successfully applied to different scenarios. Atmospheric imaging and long-distance underwater imaging are faced with the problem of how to effectively collect and interpret the scattered light. The traditional analysis method of atmospheric optics is for ballistic light. To achieve efficient acquisition, the acquisition method for scattered light must be used, such as shower-curtain and synthetic aperture. To achieve interpretation, the speckle correlation must be guaranteed, which requires high-speed, small NA optical system. Another important issue is the ambient scattering light. The possibilities to remove atmospheric ambient scattering under passive conditions may include the need to reduce the depth of field, such as confocal and synthetic aperture methods. In a sense, the most direct way to enhance imaging quality is to improve the performances of the cameras and the optical setup. When the bit depth of the camera is further increased, it is possible to address the weak signal on a large background. A faster CCD can capture the dynamic speckles with higher contrast and correlation. Multi-position recording and binocular viewing configurations, assisted by human-visual system, may present a novel scheme to enhance the capability of the long-range optical imaging. In addition, the improvement of instruments and computing ability is helpful for us to better analyze the influences of various factors in the atmospheric environment. After taking all these considerations into account and enhancing the signal imaging from the background, it is possible to extend the human ability to acquire long-range optical image from atmosphere or underwater.

5 Some ways to use chaotic light fields for the inspection of various depth-extended media (Wolfgang Osten, Stephan Ludwig, Giancarlo Pedrini, Johannes Schindler, Alok Kumar Singh, Mitsuo Takeda)

5.1 Status

Scattering media are an ongoing challenge for all kind of imaging technologies including coherent and incoherent principles. They have always been considered as challenging

objects for imaging and inspection. Imaging through random media has been matter of research for more than 50 years [58, 59]. Inspired by new approaches of computational imaging and supported by the availability of powerful computers, spatial light modulators, light sources and detectors, a variety of new methods ranging from holography to time-of-flight imaging, phase conjugation, phase recovery using iterative algorithms and correlation techniques have been introduced and applied to different types of objects such as tissues, foam materials, turbulent and translucent media [13, 16, 17, 22, 60–65]. However, their applications are often limited to two-dimensional imaging. On one hand the inspection of depth-extended objects is still a challenge. On the other hand the systematic use of scattering media could allow the implementation of a new type of cameras [13], sensors [66] and microscopes [23] by use of a simple scatter plate instead of a conventional objective lens. In the following, we report about our recent findings in this field. First, we describe how to explore depth-extended objects by means of a scattering media [6]. Afterward, we extend this approach by implementing a new type of a microscope making use of a simple scatter plate as a kind of a flat and unconventional imaging lens and show how to magnify complex objects with diffraction-limited resolution this way [23]. This kind of microscope allows to be transformed into a single-pixel imaging tool [67]. Finally, we describe our shearing interferometer in combination with structured illumination for retrieving the axial position of fluorescent light emitting spots embedded in scattering media [68].

5.1.1 Exploring depth-extended objects by use of a scattering media

Since the early work in the 1960s by Goodman et al. [58], many methods have been proposed for imaging through diffusing media. These methods have a potentially wide range of applications from biomedical to astronomical imaging. Thus, imaging through an opaque diffusing medium with diffraction-limited resolution has become an important academic and technical challenge as well. One straightforward strategy is imaging with ballistic photons selected either by coherence gating as in optical coherence tomography [69], time gating as in femto-photography [62], or holographic gating [60]. Because only a limited number of ballistic photons are used (with scattered photons being wasted) and also because the sequential scanning of the gate window is required, these methods are used mostly for imaging of static objects through a weakly scattering medium. A way to make use of the diffused light is to implement unconventional imaging techniques that are insensitive to phase perturbations. Among these are photon correlation holography [70], and coherence holography [71] that can image through a dynamic diffusing media. But they are not lensless systems. Freund proposed in 1990 a lensless imaging technique based on speckle intensity correlation, in which he regarded a diffuser as a useful imaging device and made use of his discovery of the memory effect [72, 73]. This idea was further developed by other researchers as for instance by Bertolotti et al. [16] who reported an angular correlation technique that can avoid prior calibration with a reference source (which was necessary in Freund's scheme). Katz et al. [17] proposed another reference-free method and showed that the intensity autocorrelation of the scattered light is identical to the autocorrelation of the object image itself and that the object can be reconstructed using a phase-retrieval algorithm. However, these intensity correlation techniques were demonstrated only for two-dimensional (2D) images because of their intrinsic property of infinite depth of focus [72].

In his seminal papers, Freund proposed a lensless imaging technique in which he regarded a diffuser as a useful imaging device and named it wall lens. Extending this idea, we made use of the turbid medium as a virtual imaging lens. We exploit the potential of the virtual imaging lens for 3D imaging, so that it can create an image of 3D objects with variable focusing and controllable depth of focus. To avoid the computational burden of a 3D phase-retrieval algorithm and the restricted field of view incidental to image recovery from the autocorrelation, we modify the intensity correlation technique and introduce a reference point source near the object. The reference point source, which is incoherent with the object illumination, has the role of a guide star in a manner similar to Goodman's interferometric imaging [74]. The use of a reference source may set a certain restriction in some applications but provides a much simpler solution as those based on the autocorrelation combined with an iterative phase-retrieval algorithm. Our solution is free from iterative phase retrieval, gives a wider field of view, and permits direct 3D image reconstruction from the cross-correlation between the intensity distributions on a pair of planes axially separated in the scattered fields. Detailed information about the principle is given in [6]. Figures 6 and 7 show the setup and the experimental evaluation respectively.

5.1.2 Diffraction-limited microscopy with a simple scatter plate

For many centuries, imaging has been dominated by the performance of lenses. A lot of research has been done for this conventional kind of imaging, and sophisticated lens design for applications such as photography, microscopy and lithography has created a big market for industry. Different methods have been tried, but there is up to now not an alternative to conventional lenses in sight. High-resolution imaging has been one field where the demand for high-quality lenses is constantly increasing, especially for microscopes where the

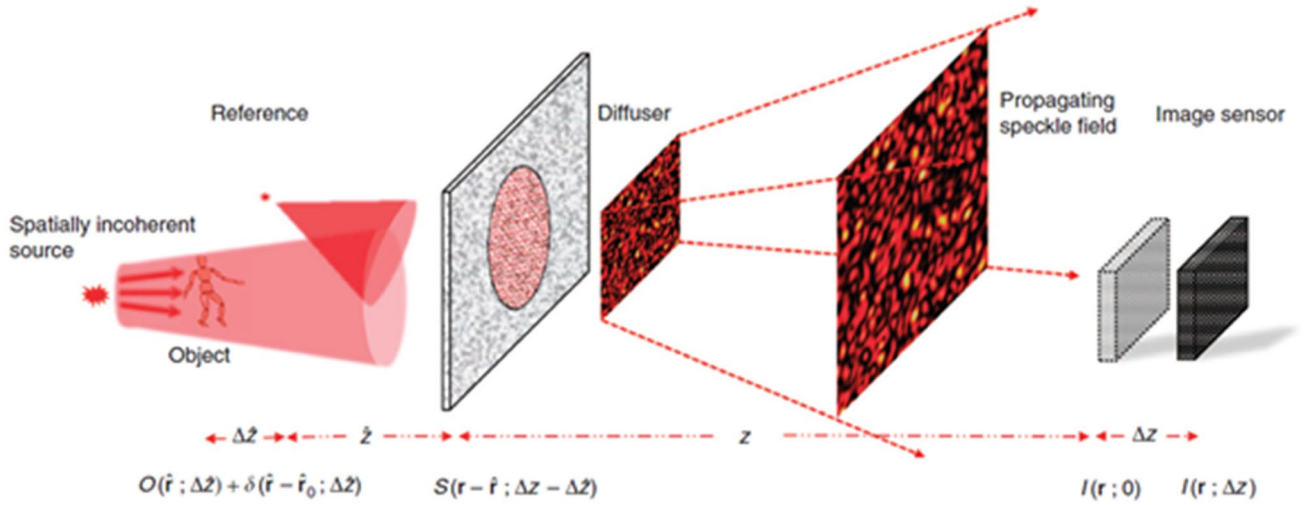

Fig. 6 Depth-extended imaging using a diffusing medium: sketch of the experimental setup. A diffusing object O is placed at a distance $\hat{z}+\Delta\hat{z}$ from a diffuser S and is illuminated by a spatially incoherent narrowband light source. A reference point source δ, which is incoherent to the object beam and is laterally shifted by $\hat{\mathbf{r}}_0$ from the object, is placed in the reference plane at a distance $\hat{z}$ from the diffuser. Speckle intensities are detected by an image sensor at distances z and $z+\Delta z$ downstream from the diffuser

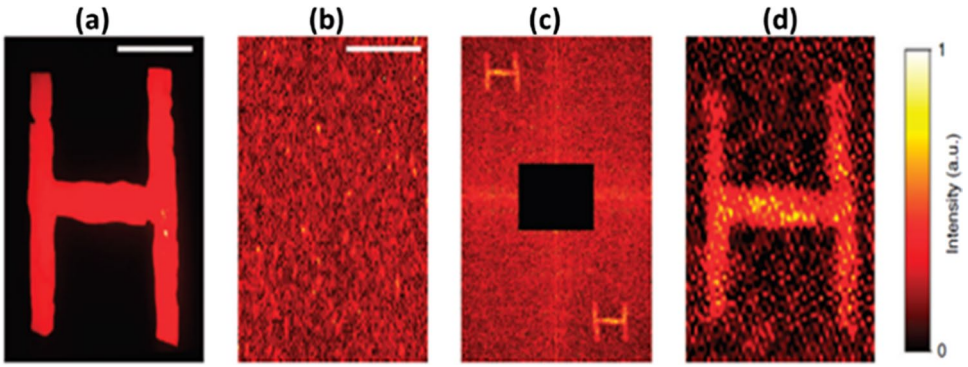

Fig. 7 Chicken breast tissue or imaging system: a 1.5-mm-thick chicken breast tissue sandwiched between two glass slides was used as a diffusive medium. Non-invasive imaging of the 'letter H' using a spatially incoherent light source was performed through this biological tissue. **a** The object, 'letter H' (500×330 μm) **b** part of the recorded speckle pattern, **c** the autocorrelation, and **d** the reconstructed object. The scale bars in a, b are 150 μm (20 pixels) and 447 μm (60 pixels), respectively

quest for high-definition objective lenses is unbroken. One consequence of this challenge are the continually increasing complexity and prices of objective lenses. Traditionally lens-based microscope objectives have fixed focal length, high numerical aperture, short working distance, limited depth of focus and magnification, which often sets restrictions in their application. The correction of aberrations for microscope objectives requires an extended design consisting of a certain number of spherical and aspherical lenses (sometimes more than 10), which increases complexity, bulkiness, and price.

We developed an alternative imaging systems which is based on Freund's intensity correlation technique [71], which permits lensless imaging of an object using a scattering medium by utilizing its memory effect. Specifically, we propose a new imaging device called 'scatter-plate microscope' in which a conventional objective lens is replaced by a simple scatter plate [23]. The scatter-plate microscope has the following unique characteristics that are not available with traditional microscopes:

- extremely thin and light (suitable for low-cost production),
- variable focal length and magnification (self-adaptive to any conjugate image planes),
- variable NA and field of view,
- flexible working distances extendable as desired,
- compatible in reflection and transmission modes,

- immune to phase disturbances and aberrations,
- easy to fabricate with scalability in device size, robust to environmental changes.

Thus, a single low-cost scatter plate can perform the tasks of various microscope objectives with different magnifications, NAs and focal lengths. A relatively wider field of view (FOV) and variable depth of focus (DOF) are exclusive features of the presented technique. Our cross-correlation based technique, combined with a reference point source, is capable of imaging complex objects. We successfully performed microscopic imaging using scattering plate on technical as well as biological samples, Fig. 8. We could easily obtain a resolution of 2.19 µm. It also opens up the possibility of utilizing the scattering media as imaging lenses for X-ray and ultraviolet radiation. Thus, we implemented a technique that can turn a costless scattering surface into a high-resolution microscope objective.

5.1.3 Single pixel scatter-plate microscopy

If the scattering behavior of the scatter plate is known, the point-spread function PSF can be retrieved from diffraction theory. Therefore, by replacing the scattering media by a spatial light modulator (SLM), displaying some pseudo-random modulation pattern, the recording of the PSF becomes entirely redundant. Moreover, this approach allows transforming the scatter-plate microscope into a single-pixel imaging tool [67]. A single-pixel detector measures the intensity signal generated with many different pseudorandom modulation patterns. For each pattern, the PSF is now retrieved from diffraction theory. Image retrieval is subsequently realized by calculation of the ensemble cross-correlation between the measured intensity signal and the PSFs. Figure 9 demonstrates image retrieval by the single-pixel scatter-plate microscopy with modulation patterns displayed by a digital micro-mirror device (DMD).

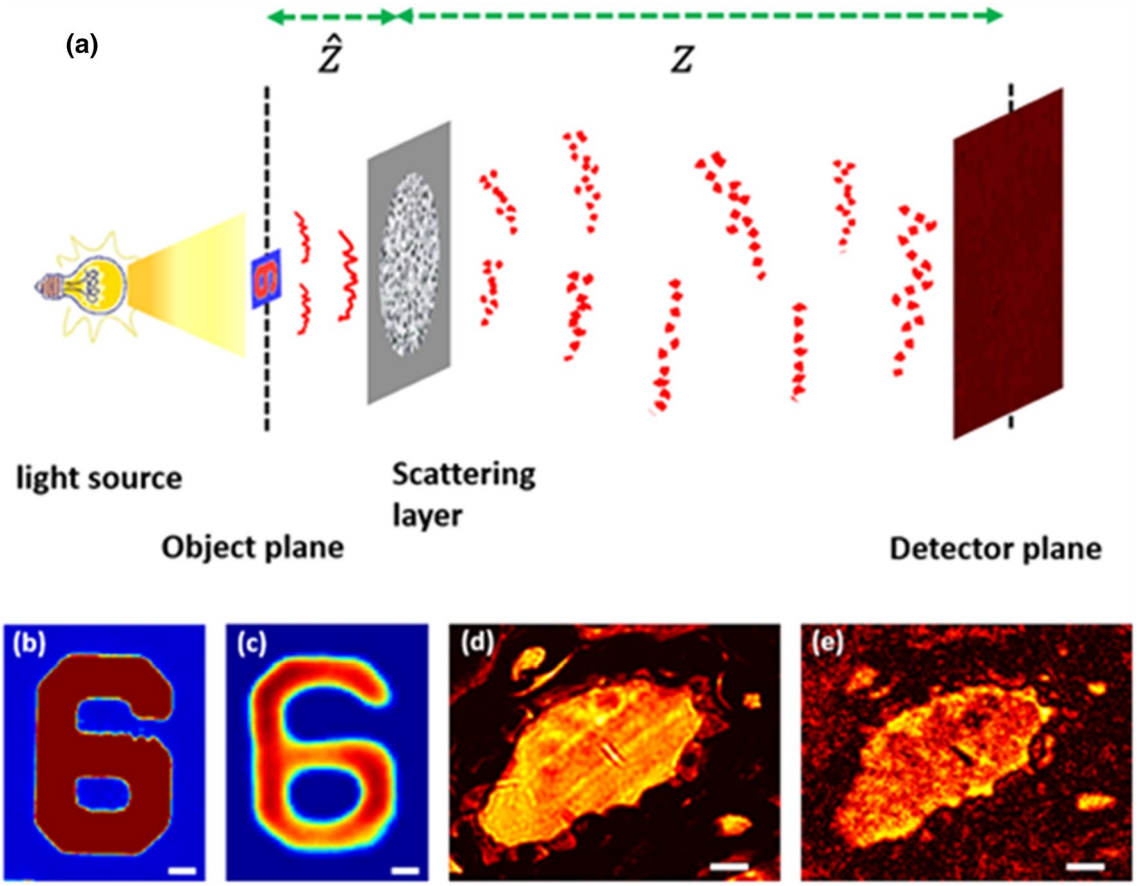

Fig. 8 Scatter-plate microscopy: principle and examples. **a** Principle: the object is placed close to the scattering layer at distance $\hat{z}$, and the aperture size is increased to achieve a high numerical aperture. The image plane is far at a distance z from the scattering layer. The conventional microscope image made with monochromatic illumination of the Fig. 6 from a USAF test target and a section of pine wood stem are shown in **b** and **d**. Their corresponding images taken with a scatter-plate microscope are shown in **c** and **e**, respectively. The scale bar in **b** and **c** is 3 µm, and in **d** and **e** 20 µm in object space

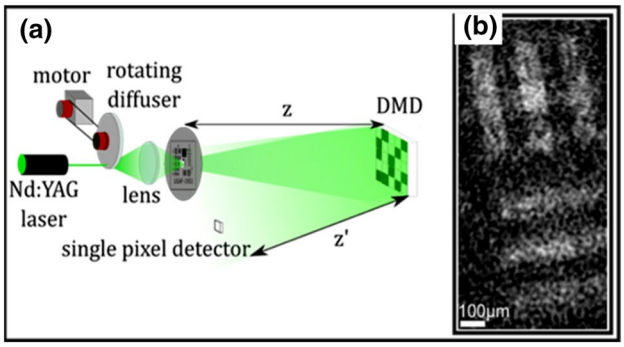

Fig. 9 Single pixel scatter-plate microscopy. **a** Setup. The monochromatic, spatially incoherent sample illumination is generated by leading a laser beam through a rotating ground glass diffuser. A digital micro-mirror device (DMD) displays many different pseudorandom modulation arrays. For each scattering array, the intensity in the scattering field is measured with a single-pixel detector. Image retrieval is realized by calculating the ensemble cross-correlation between the measured single-pixel signal and the computationally generated PSFs of the modulation arrays. **b** Image of group 2 element 2 of the USAF test target retrieved by single-pixel scatter-plate microscopy. 14,000 pseudorandom modulation arrays were displayed by the DMD

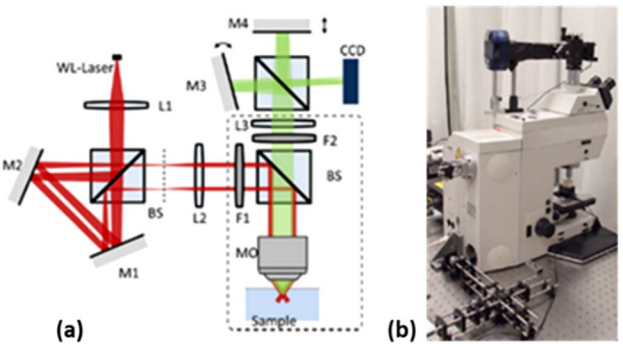

Fig. 10 **a** Schematic layout and **b** photograph of the experimental setup. Ls, Lenses; Ms, mirrors; BS, beam splitters; Fs, band-pass filters; MO, microscope objective. The dashed line corresponds to the housing of the microscope

5.1.4 Depth-resolved detection of fluorescent light emitting particles embedded in a scattering medium

Microscopy methods for noninvasive diagnostics are limited by the strong scattering encountered in biological materials. This leads to disturbing background signals, weak signal-to-noise ratio, and image degradation. The situation is even worse when one needs to determine dimensional information about the position of a signal source in all three spatial dimensions. Light from infocus as well as from regions far out of focus contributes to the recorded signal. Hence, some sort of discrimination between the desired signal and contributions arising from scattering in the rest of the sample is needed. Many diagnostic applications require such dimensional measurements: in the classification of skin cancer, the extent of a tumor in the vertical direction is directly linked to its development over time [75]. Hence, three-dimensional (3D) data about the location of certain structures, in particular along the z-axis, could contribute to a better classification of images, the recognition of features, and the automated segmentation of malign and benign areas. In applications where optical methods aid in the determination of tumor margins or even serve as feedback during surgery, dimensional information is obviously of crucial importance.

Here, we show a phase-sensitive method for the depth-resolved detection of fluorescent light based on the combination of structured illumination with an interference pattern arising from two intersecting beams with shearing interferometry for depth detection [68]. This aims at combining the advantages of fluorescence detection and using highly sensitive interferometric signals for the depth evaluation. In addition to using fluorescence band-pass filters, the contribution of scattered light is suppressed by locally addressing the excitation of fluorescent light and limiting the excitation volume by the geometry of the illumination setup. The implementation of a phase-shifting procedure allows efficient separation of the interferometric signal from the incoherent background, which is of particular importance for recording signals from a scattering environment. However, this comes at the expense of an increased time for image acquisition as at least three phase-shifted images have to be recorded. While the setup has a similar structure as some holographic methods, the focus of this work is the measurement of the axial position of a fluorescent light source in a scattering environment rather than imaging. In contrast to scanning methods such as confocal or multiphoton fluorescence microscopy, signals arising from regions far out of focus can be used, so scanning along the vertical direction is avoided. The lateral shearing is implemented in a Michelson interferometer with a tilted mirror that is integrated into a conventional microscope.

The experimental approach relies on combining a dedicated illumination setup with a shearing interferometer for the phase reconstruction. The basis for the setup is a usual fluorescence microscope in epi-illumination configuration, see Fig. 10. The band-pass filters F1, F2 are adapted to the fluorophor rhodamine 6G with absorption and emission peaks at 532 nm and 552 nm, respectively. To preserve the flexibility with respect to a working distance covering several hundred micrometers, a microscope objective with moderate numerical aperture of 0.4 and 20 × magnification is used. The creation of an interference pattern in the focal plane can be achieved by illuminating with two beams separated in the pupil plane of the microscope. This leads to two light cones intersecting each other under an angle in the focal plane after passing the microscope objective.

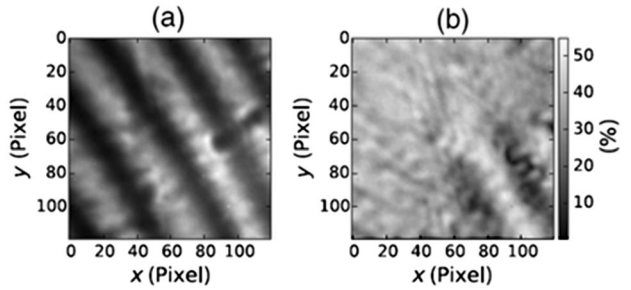

Fig. 11 Raw fluorescent intensity image with **a** interference pattern and **b** fringe contrast for fluorescent layer at a depth of 550 µm

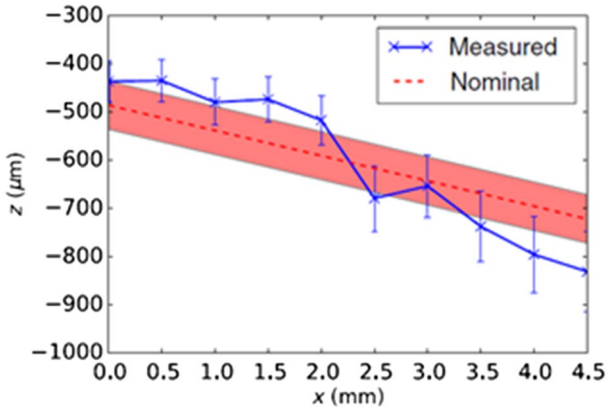

Fig. 12 Validation of depth reconstruction at a fluorescent layer

Translating one of the mirrors M1, M2 in axial direction allows the adjustment of the intersection angle.

The principle of phase reconstruction and the estimation of the resolution are given by Schindler et al. [76]. The wave fronts are modeled as spherical wave fronts that can be expanded into Zernike polynomials. For experimental verification spatially extended fluorescent light sources and a measurement range of several hundred microns in a weakly scattering material are considered. In this configuration, a scattering phantom with isolated inclusions of fluorophors is examined. The sample contains a layer of fluorescent material with at thickness of 10–15 µm, which is tilted by 3° with respect to the surface. Hence, different lateral positions of the sample correspond to different depths of the fluorophors. Figure 11 shows the raw signal of a depth of 550 µm and the corresponding fringe contrast. In spite of the large extent of the fluorescing volume and the lack of spatial incoherence, an interference pattern with a fringe contrast in the range of 30% is recorded. It is assumed that this is due to the illumination, which confines the excitation of fluorescent radiation both laterally and axially. This is also in agreement with previous simulation results [76] where the propagation of the excitation and the fluorescent light has been modeled based on numerical solutions of the Maxwell equations and similar values for the resulting fringe contrast have been obtained. Figure 12 shows the comparison between the nominal values and the result for the reconstructed depths for different positions along the profile. The reconstructed values agree with the nominal ones within the range of the uncertainty for the actual layer, corresponding to a relative error of around 10%. It is to be noted that no spatial coherence is required in the formation of the shearing interference signal, as interference takes place between parts of the wave front emerging from the same point in space. The sole effect of an extended source distribution is a decrease in contrast.

5.2 Conclusion

Here, we presented several approaches for the utilization and the inspection of scattering media. First, we described how to explore depth-extended objects by means of a scattering media. Afterward, we extended this approach by implementing a new type of microscope making use of a simple scatter plate as a kind of flat and unconventional imaging lens. This kind of microscope allows to be transformed into a single-pixel imaging tool. Finally, we introduced our shearing interferometer in combination with structured illumination for retrieving the axial position of fluorescent light emitting spots embedded in scattering media. Part of this work was already published in [77].

6 Randomness assisted digital holography (Rakesh Kumar Singh, and Tushar Sarkar)

6.1 Status

Digital holography (DH) offers a significant advantage in different walks, from medical diagnosis to metrology, due to its ability to record and reconstruct the complex fields of light [78]. This unique feature of the DH is widely utilized to build fast, non-destructive, full-field, three-dimensional (3D), and high-resolution quantitative phase imaging (QPI) systems [78–82]. The DH is an interferometric technique and records an interference pattern of the light coming from the imaging beam with a reference wave, and the hologram is digitally recorded by an intensity detector. The recorded interference pattern is subjected to a digital back-propagation by using different propagation algorithms. This helps to implement 3D reconstruction and digital focusing without using any mechanical means. Due to its interferometric principle, various designs and developments in interferometry have been utilized to configure experiments in the DH. Some important DH schemes are in-line, off-axis, and phase-shifting holography [78–82]. The off-axis holography demands a carrier beam to avoid the twin image problem of

the in-line holography. Significant attempts have also been made to synchronize the DH with the microscopy to tackle limited depth of focus in a high numerical aperture imaging system and attain the high magnification ratio desired in the conventional optical microscopy [83, 84]. On the other hand, the idea of recording and reconstructing information from self-luminous or incoherent objects has introduced new trends in holography [85, 86]. The strong theoretical basis of the coherence theory has been extremely useful and offered a framework to develop new advances in holography with the arbitrary coherence light sources [87].

When the object is obscured by the random scattering medium or illuminated by a random light, direct imaging of a non-stochastic complex-valued object is a challenging task. Propagation of the random light leads to scrambling in the space and hence no direct resemblance with the object. This is a challenging, yet practical problem leading to the conventional holography nearly ineffective. The information available at the detector plane is a random and seemingly information-less pattern. These issues have been widely investigated by using adaptive optics, phase conjugation, iterations [88–90]. Issue of imaging from the random light can be broadly categorized into two. First is a situation where the random light is by choice or desired such as in the correlation holography, speckle-field digital holography, and ghost imaging [11, 85, 91–93]. The second category covers examples, where desired information is spatially scrambled due to propagation of light through a random scattering medium and examples are imaging through atmospheric turbulence, scattering wall, shower-curtain effect, etc. [17, 88, 94, 95]. The existence of the random field in two different categories, albeit for different reasons, can be treated in a common framework of the coherence theory and the holography based on the correlation function offers a great potential. The foundation of such unconventional holography, called correlation holography, is derived and based on the close analogy between the complex coherence function and the optical field [96, 97]. Moreover, central results of the coherence theory such as the van Cittert–Zernike theorem and the Hanbury Brown–Twiss (HBT) approach have played significant role in the development of such unconventional holography [98].

6.2 Current and future challenges

The correlation holography can be applied to image generic objects from random light. In contrast to direct imaging in the DH, correlation holography requires experimental measurement of the complex coherence functions. This is possible by using a suitable interferometric setup to measure a two-dimensional complex coherence structure preferably from a single measurement for imaging of a dynamic object [94–98]. A configuration of the experimental geometry with the HBT approach is shown in Fig. 13a. This system is designed to implement an unconventional holography with the coherence waves (rather than the optical field). The object information is scrambled and propagates to a charged coupled device (CCD) plane [94, 95]. The second-order correlation of the random field, i.e., coherence function, carries information of the object. However, direct measurement of the complex coherence function is not possible from a single arm. Therefore, a reference coherence wave with desired correlation structure is inserted in the experiment by illuminating a reference ground glass with the point source. The intensity correlation of the resultant random pattern at the CCD in the Fig. 13 is expressed as the modulus square of the superposition of the coherence waves [95]. This relation has a close analogy with the conventional holography where interference of the optical field is used. An off-axis strategy helps to reconstruct the object information from a single measurement of the random pattern [95]. Furthermore, if we consider that the optical field at the plane of scattering is

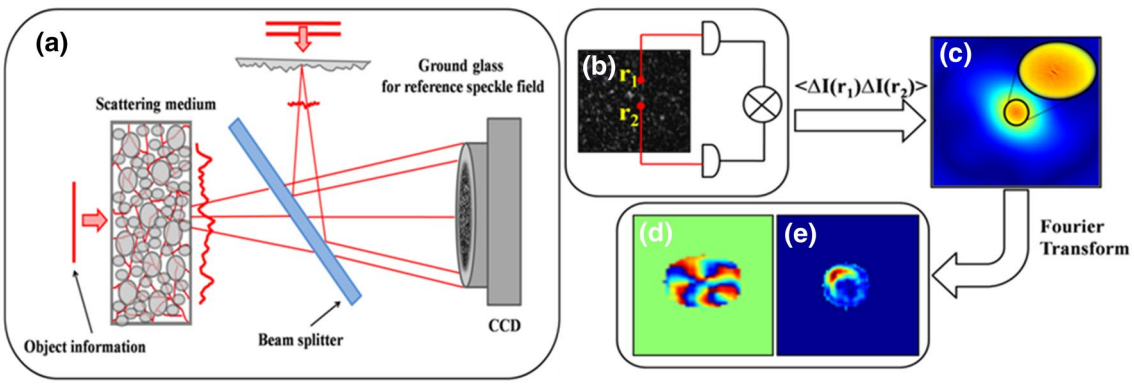

Fig. 13 Schematic of scattering assisted holography method. **a** Sketch for holography with coherence waves. **b** Recorded speckle pattern. **c** Cross-covariance of the speckle. **d**, **e** reconstructed amplitude and phase distribution of vortex beam of topological charge $l=5$ from cross-covariance using Fourier fringe analysis

an interference pattern encoding object, then the coherence holography reconstructs a complex-valued object. Here, we consider a Fourier hologram encoding the vortex structure is located behind the random scattering medium. The holography with the HBT approach in Fig. 13a permits the realization of lensless imaging and recovery of the Fourier hologram from a random light. Consequently, reconstruction of the hologram provides a complex field of the object located behind the scattering medium.

Successful reconstruction in the coherence holography depends on the validity of the assumption of spatial stationarity and Gaussian statistics of the random field at the detector [95]. The full-field reconstruction is also restricted if spatial stationarity is available only in the patches. The limitation of spatial stationarity can be removed by appropriate selection of the propagation kernel, say a Fraunhofer. It is possible to achieve spatial stationarity in the Fresnel domain by using an appropriate interferometer [95]. Another challenge in correlation holography is spatial resolution due to the finite correlation length of the scattering medium. Some of the existing challenges can be addressed by combining the computational methods with correlation holography such as deconvolution, and digital phase-shifting [96–99].

6.3 Advances in science and technology to meet challenges

The challenge to image from the randomness employing correlation optics, although there have promising results and new directions, still demands some key scientific and technological progress. One possible strategy to successfully meet such demand is to further explore analogy and connections between the optical field and complex coherence. Such a strategy will provide opportunities to import existing technological innovations and the development of coherent optics to the experimental realization of ideas in the coherence theory. Furthermore, the combination of available theoretical frameworks of the coherence optics with experimental optics will provide a new research direction for experiments with a generic light source and in developing unconventional imaging methods [94–99]. A close analogy between space and time is also useful to reconstruct the temporal modulation from randomness. This connection has led to intentional and significant interests in unconventional imaging in the temporal domain. Therefore, the combination of spatial and temporal is desired to implement spatio-temporal unconventional imaging systems. Availability and progress in the development of high-speed temporal detectors and plug-in and plug-out arbitrary coherent sources are expected to significantly contribute to the progress of unconventional imaging methods such as correlation holography, ghost imaging, etc.

6.4 Concluding remarks

The development of holography with coherence waves and its applications for imaging from random light have demonstrated new trends in holography. Moreover, this also highlights the enormous potential to combine the technological progress of the conventional holography with the theoretical resources of the coherence theory. The key features of such unconventional holography utilize the randomness of the light and opens new avenues for quantitative imaging.

7 Quantitative phase imaging with spatially partially coherent sources (YoonSeok Baek, Hervé Hugonnet, KyeoReh Lee, and YongKeun Park)

7.1 Status

Label-free imaging techniques have become a powerful tool in biomedical science by addressing issues of using exogenous labeling agents. Instead of using fluorescence proteins or stains, label-free techniques produce image contrast by exploiting elastic and inelastic light scattering. For this reason, label-free imaging is inherently non-invasive and free from phototoxicity. Among various techniques, quantitative phase imaging (QPI) is a unique method that measures optical phase delay induced by biological specimens. Over the last decade, QPI has emerged as an invaluable tool for cell biology and pathology because the optical phase accurately reflects the morphology and internal structures of a transparent sample [100]. QPI provides both two- and three-dimensional imaging modalities. The two-dimensional (2D) QPI is a full-field method that quantifies a spatial change in phase at the focal plane. By providing sub-nanometer sensitivity in optical path length, 2D QPI enables the monitoring of cellular structures and dynamics under various pathophysiological conditions [101]. The three-dimensional (3D) QPI, or optical diffraction tomography, produces a refractive index tomogram by solving an inverse scattering problem using optical fields measured at different incident angles. Such a tomographic approach decouples a refractive index and thickness of a sample, which are indistinguishable in 2D phase delay images. Accordingly, 3D QPI allows quantitative analysis through biological and morphological parameters, such as dry mass, protein concentration, volume, surface area, and sphericity [102].

This short review focuses on QPI with spatially partially coherent sources. In the following sections, we outline challenges associated with spatial partial coherence and discuss recent technological progress made in QPI.

7.2 Challenges in QPI using coherent light

Conventional QPI techniques have been based on holography which requires a coherent source and a stable interferometer. However, as the field of QPI finds its application in biomedicine, there has been a growing need for the simple implementation of QPI outside well-controlled optical laboratories. In this regard, one major challenge for QPI is to utilize spatially partially coherent light. By embracing spatial incoherence, QPI can be realized in widespread optical microscopes and can improve phase sensitivity by suppressing coherent speckle noise. However, the partial coherence is incompatible with most QPI techniques because it is challenging to measure phase delay images based on interferometric techniques that use reference beams. Despite the efforts to reduce speckle noise using various approaches exploiting spatial compounding or machine learning approaches [103–105], the presence of speckle noise is inevitable when a coherent light source is used.

Such an issue can be addressed by interfering partially coherent light. For example, phase-shifting interferometry can be employed by changing the relative phase between the unscattered and scattered components of light using a spatial light modulator [106]. Resulting intensity images are equivalent to phase-shifting interferograms from which phase delay images are obtained. Alternatively, it is possible to induce interference between the partially coherent light and its spatially translated copy using diffractive masks to produce phase-gradient images [107, 108]. The main advantage of these common-path approaches is the compactness of setups that can function as add-ons to optical microscopes. However, their phase measurements are less accurate than conventional QPI because phase images are vulnerable to halo artifacts [106], the spatial coherence of the illumination [8], and the paraxial approximation [108].

7.3 Advances using incoherent light to meet challenges

Recently, non-interferometric approaches have shown that the change in the illumination alone provides enough information to conduct QPI through analytic expressions and computational algorithms [109–111]. Unlike previous techniques, non-interferometric QPI works by controlling the illumination patterns without requiring special optical components in the imaging path of conventional optical microscopes. Among these new techniques, a set of deconvolution techniques have demonstrated 3D QPI with spatially partially coherent light. It assumes that intensity transmitted through a transparent sample is the sum of the convolution of the real part of a scattering potential and the phase transfer function, and the convolution of the imaginary part of the scattering potential and the amplitude transfer functions [112, 113].

In experiments, refractive index tomograms are reconstructed through the deconvolution of intensity images under various illumination patterns and the axial scanning of a sample (Fig. 14). The amplitude and phase transfer functions vary depending on the illumination and determine which information is retrieved from the intensity images. Therefore, it is important to optimize partially coherent

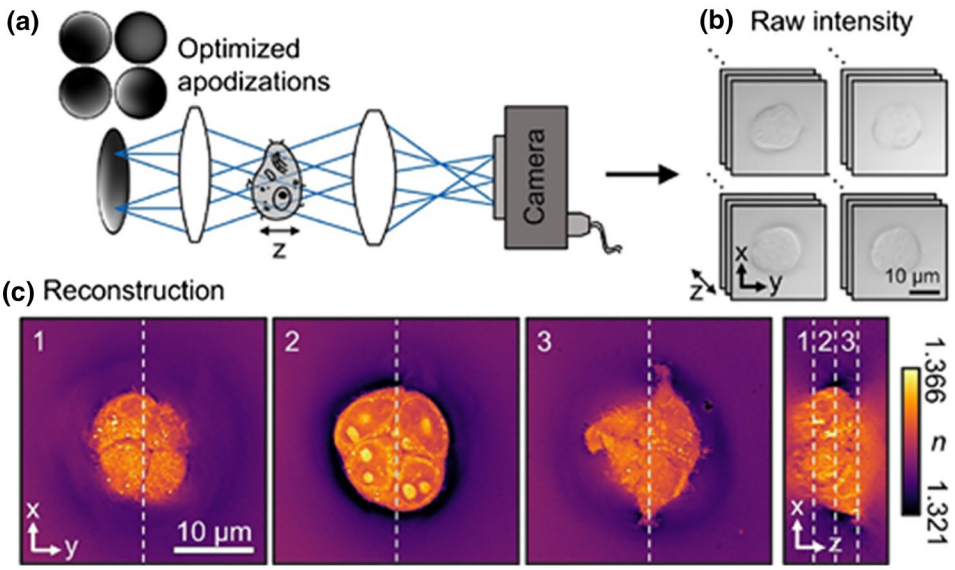

Fig. 14 Schematic of deconvolution-based 3D QPI. **a** Schematic for illuminations and axial scanning of a sample. **b** Measured intensity images for different illumination patterns and axial positions. **c** Refractive index tomogram obtained after deconvolution. Reproduced with permission from [115], OSA

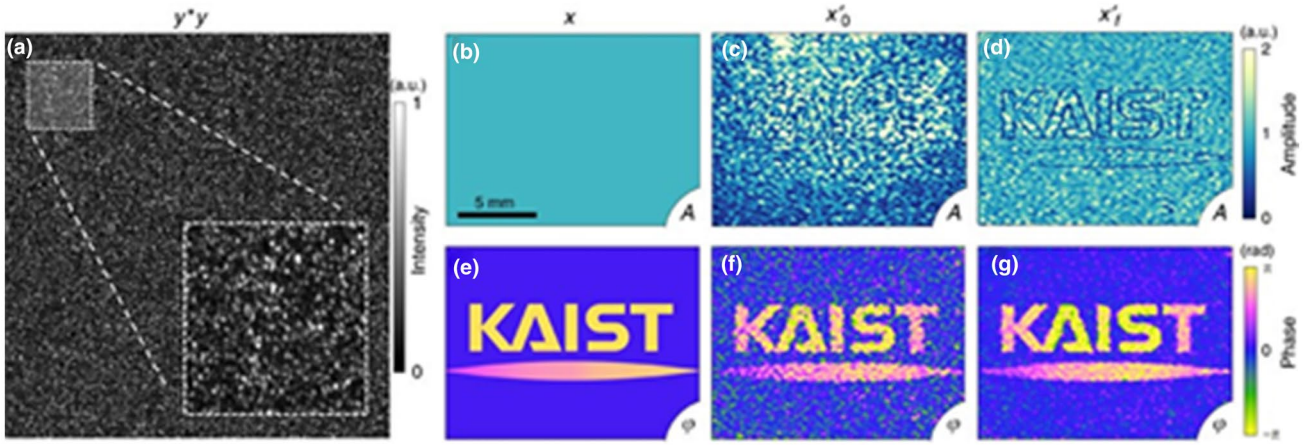

Fig. 15 Holographic imaging using speckle-correlation scattering matrix. **a** Measured speckle image. **b**–**g** Amplitude and phase images of incident light (**b**, **e**), SSM (**c**, **f**), and SSM followed by an iterative algorithm (**d**, **g**), respectively. Adapted from [5], CC-BY-4.0

illumination to obtain reliable refractive index tomograms. For example, without the axial scanning of a sample, the transfer functions need to vary sharply in the z-direction to obtain volumetric information at a focal plane. In such a case, optimized patterns become chaotic and sparse illumination [114]. On the contrary, when the sample is scanned axially, it becomes essential to obtain cross-sectional information without losing transverse resolution which is achieved with smooth illumination patterns [115]. For these partially coherent approaches, one of the remaining future challenges is to improve their accuracy beyond weakly scattering objects.

Another possibility for QPI is to exploit randomness for phase measurement. Speckle-correlation scattering matrix (SSM) is a recently developed method for holographic imaging [5, 116]. SSM utilizes the randomness of complex Gaussian variables to recover the complex amplitude of light from a speckle pattern generated by a scattering layer (Fig. 15). Its principle is based on the fact that a random scatterer generates a unique speckle pattern for different incident light. SSM has already demonstrated its potential for QPI [117], although with coherent light. Importantly, the principle of SSM has been extended to two orthogonal polarization states [118], suggesting the possibility of partially coherent QPI. The main current challenge is to develop scattering layers and algorithms for the processing of partially coherent speckle patterns using SSM.

7.4 Concluding remarks

Embracing partial coherence is the key to improve the accessibility of QPI and to facilitate the application in various biomedical contexts. Recent advances in the field suggest new possibilities to realize QPI with spatially partially coherent light.

8 Deep learning in imaging through turbid media (Wanqin Yang and Guohai Situ)

8.1 Status

Despite of great importance to imaging through turbid media in numerous applications, ranging from astronomical observations to biomedical imaging through turbid tissues, it is rather challenging and arduous to form a clear image with randomly scattered light. The difficulty lies in the fact that when light travels in a disordered medium, the wavefront generated by a point source in the object plane will be randomly distorted due to the random refractive index variations within them, which prevents the formation of converged Airy spots in the image plane as in traditional optical imaging systems. Fortunately, with the great progress of computational technology and development of related theories, many new imaging methods have emerged recently. Among them, the typical imaging methods include imaging with ballistic photons, wavefront shaping method, optical phase conjugation, transmission matrix, and optical memory effect. Additionally, ultrasound is often used as an important tool in combination with optical imaging method due to its deeper penetration depth inside biological tissues, such as ultrasound-assisted tomography and photoacoustic imaging. However, all of them are faced with different limitations and are only suitable for some specific scattering imaging scenarios. For example, iterative wavefront shaping method or transmission matrix requires long-time acquisition and cannot be applied to dynamic turbid media; while optical memory effect cannot cope with optically thick scattering media and at the same time the field of view is quite limited. Until now, imaging through thick or dynamic turbid media with high-quality reconstructions has always been the long-time pursuit.

8.2 Current and future challenges

Recent advances in deep learning (DL) have shown great potential and capability to meet the aforementioned challenges thanks to their high performance. Deep neural networks (DNN) consist of an input layer, multiple hidden layers and an output layer [119]. The input layer and the output layer are determined by the current mapping problem, while the hidden layers can be adjusted artificially. Because of the excellent fitting ability, DNNs are good at solving highly ill-posed problems. Up to now, DL has found its widespread applications in various computational imaging scenarios, to name a few, digital holography reconstruction [10, 120], computational ghost imaging [121], phase imaging [122], imaging through scattering media [27, 123]. When it comes to imaging through turbid media, it is to solve the inverse problem from the raw data buried with noise to original object information.

Lyu et al. constructed a hybrid neural network (HNN) to realize scattering imaging through a 3 mm-thick white polystyrene plate with its optical thickness equal to 13.4 [27]. Later, to improve the robustness and generalization of the neural network, Le et al. used four diffusers when collecting the training set and tested with untrained raw speckles generated from unknown diffusers, which requires the unknown diffusers to have similar statistical properties and the objects to be simple [124]. Although the speckle pattern generated when coherent light passing through static diffusers are spatially randomly distributed, the morphology of it is explicitly object-dependent, which reveals unique features of labeled images in the training set. However, when illuminated with an incoherent light, according to the statistical analysis of speckle, the incoherent superposition of numerous high-contrast speckle patterns will yield milky patterns that are almost visually indistinguishable. Furthermore, imaging through nonstatic turbid media is more challenging because of the unpredictable multiple scattering path fluctuations with time. Lately, Zheng et al. proposed a method to achieve single-shot incoherent imaging through highly dynamic and optically thick turbid media by using an end-to-end DNN [125]. In their work, the optical thickness of the tank of turbid media is as high as 16, and the corresponding decorrelation time is about a few hundred microseconds.

So far, almost all the deep neural networks proposed for computational optical imaging employ a supervised training strategy, which means the need for a large amount of paired labeled images in the training set. In scattering imaging, matched labeled images of ground-truth objects (objects on the spatial light modulator) and many blurred patterns (images recorded by the camera) are usually obtained via synchronous control of the spatial light modulator and camera. With sufficient training set, the weights and biases of neurons can be optimized, and thus yielding a well-trained network before it can be used. Despite of the huge breakthroughs in imaging through scattering media, there exist some drawbacks in DL methods. First, solely data-driven DL method has limited generalization. Since the parameters in the neural networks are all obtained by fitting the paired labeled images, the trained model is inevitably over-relying on the training set and implies some unknown features of the input. The conventional solution is to increase the diversity of training data, for example, Li et al. used a training set containing different types of raw speckle patterns from four diffusers. Second, in many practical applications, especially in biological imaging, it is rather difficult to obtain ground-truth images for supervised learning. Common methods to obtain ground-truth images mainly include high-precision optical reconstruction and preset of real objects. Obviously, it is a great challenge to realize object reconstruction from scattered photos. Meanwhile, the preset of objects is the most popular case at present, which means that it needs to invade inside or behind the scattering medium roughly.

8.3 Advances in science and technology to meet challenges

As for the limited generalization of networks and the failure to obtain ground-truth object labels, there is no particularly effective solutions at this stage. However, recent research seems to suggest that introducing physical models into DNNs is expected to overcome the problem of lack of ground-truth object in supervised learning and might also effectively reduce the dependence of the network on the training sets. To image through turbid media, Zhu et al. has proposed a method combining the physics prior with neural network [126]. By exploiting the speckle correlation prior, the efficient physics prior provides an optimized direction for the neural network to find the optimal reconstruction in different scattering scenes with improvement of feature extraction efficiency and better performance in reconstruction of hidden objects with high complexity.

Furthermore, when the physical model of the forward propagation that represents the process of image formation is known, usually there are two strategies to deal with the problem of lack of ground-truth objects, which is illustrated in Fig. 16. Learning from simulation is shown in Fig. 16a with two steps included. In step one, physical model is used to generate a large number of matched labeled images, which is aimed to optimize the DNN mapping the model-informed images to the objects via supervised training. In step two, the measured image is fed into the well-trained DNN to obtain corresponding reconstruction result. Figure 1b represents the optimization process guided by the physical model. In this case, an output delivered from the DNN will result in an estimated measurement via the physical model. Calculate the mismatch between the estimated measurement and

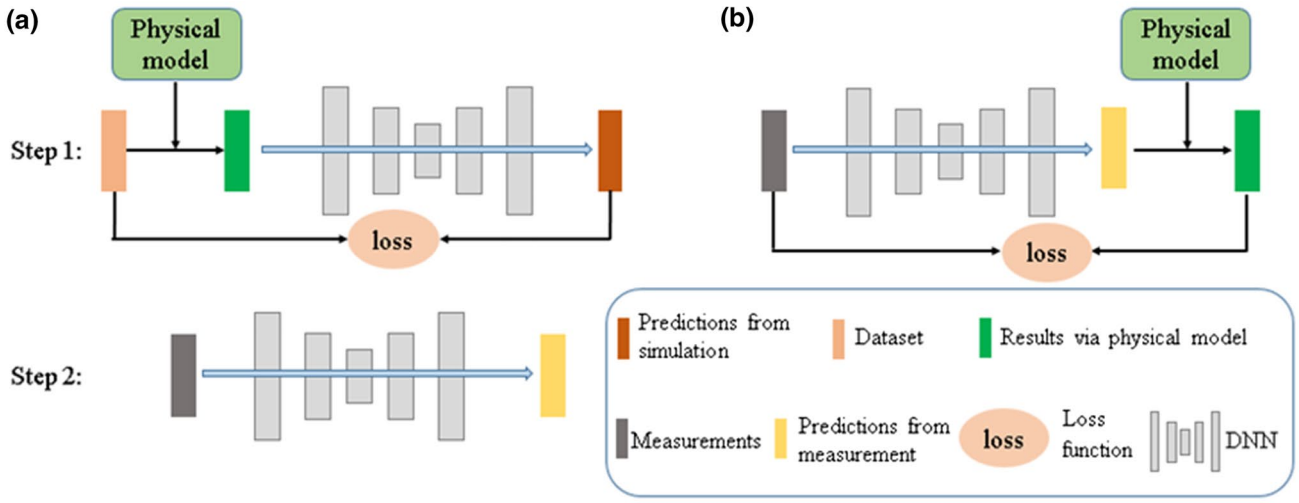

Fig. 16 Comparison of two types of physical model-based DNN. **a** Learning from simulation, **b** physical model-guided optimization solution without training

the actual measurement, then update the weights and biases in the DNN. These two strategies have made progress in computational ghost imaging and phase imaging separately, which has boosted the application of DNN based on physical models in other fields.

However, when it turns to imaging through scattering media, exact physical models corresponding to the scattering process always tend to be unavailable in practical situations. Despite the fact, recent research has inspired us as well. Johnstonbaugh et al. have proposed a method able to localize the targets below 40-mm imaging depth inside scattering medium with high precision [127]. The network is trained from the simulation-generated labels, corresponding to the strategy in Fig. 16a. It is important to determine the optical intensity distribution inside the medium because of its influences on the strength of the acoustic signals. Thus, light diffusion approximation is taken into the physical model, which can help to map the scattered light to the acoustic signals. Similarly, a forward model containing multiple scattering has been used to generate training data [128]. Then, the DNN is trained and able to recover the three-dimensional phase features of complex, multiple-scattering biological samples experimentally. As far as I am aware of, the research on imaging through turbid media based on the second strategy has not yet appeared, but there might be some in the future.

8.4 Concluding remarks

In this section, we have introduced the great achievements of supervised deep learning in imaging through turbid media and elaborated on the difficulties and challenges faced by the data-driven DNN, including limited generalization and lack of ground-truth objects. With the increasing successful applications of physical model based DL for computational imaging, we believe that physical models are efficient solutions to solve the aforementioned two problems.

9 Computational imaging for optical sensing and control through scattering media (Ryoichi Horisaki)

9.1 Status

Optical sensing and control through scattering media are longstanding and challenging issues in the fields of optics and photonics, especially for biomedicine, security, and astronomy [63, 129]. Recently, computational imaging, which is a powerful imaging framework that combines optical and computational processing as shown in Fig. 17, has contributed to these topics due to recent advances made in information science, such as compressive sensing and deep learning [130, 131]. Here, we introduce our recent research

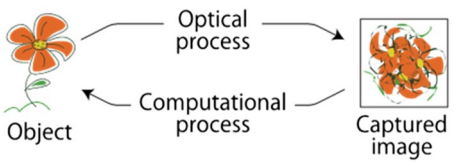

Fig. 17 Computational imaging

activities regarding computational imaging for optical sensing and control through scattering media.

9.1.1 Speckle-correlation imaging

Speckle-correlation imaging is a technique for non-invasive imaging through scattering media [16, 17]. In this method, it is not necessary to probe the optical field behind or inside scattering media. This advantage is important for practical applications. Speckle-correlation imaging exploits a shift-invariance of the scattering process, which is called the memory effect [73]. By exploiting the memory effect, the autocorrelation of a captured speckle image is approximated as that of the object. Then, the object is reconstructed from the autocorrelation by using phase retrieval [20].

We have extended two-dimensional speckle-correlation imaging to three-dimensional cases in a number of demonstrations. The so-called axial memory effect has been reported, where speckles scale laterally with the object distance [6]. In this case, the three-dimensional correlation of a depth-dependent object is calculated from the captured speckles based on the axial memory effect, and then the object is three-dimensionally recovered by three-dimensional phase retrieval for the correlation [18, 132]. Similarly, speckle-correlation imaging is extendable to spectral imaging. The spectral or chromatic memory effect also has been reported, where speckles are laterally magnified as the wavelength becomes longer [133]. A multispectral object is recovered from a speckle image through three-dimensional correlation and three-dimensional phase-retrieval processes based on the spectral memory effect [134].

9.1.2 Learning-based imaging and focusing

Machine learning, such as deep learning, has grown rapidly. This technology has contributed to various fields, including optics and photonics. In particular, computational imaging is an active area for introducing machine learning technologies to imaging systems [135]. Machine learning has enabled us to realize regression of forward and inverse processes of optical phenomena. This is important for optical sensing and control because the inverse problem plays an important role there.

We have presented learning-based imaging and focusing through scattering media [4, 29, 136–140]. In these studies, the inverse function of the scattering process was learned with a large number of input and output pairs. Then, the optical field behind or inside the scattering media can be recovered or controlled by using the inverse function. This approach has also been applied to computer-generated holography, where an optical field is controlled through free-space propagation [141, 142]. These methods for computer-generated holography are non-iterative, enabling faster hologram synthesis compared with conventional ones.

9.2 Conclusions

Recent computational techniques have changed conventional imaging modalities and have realized various innovative imaging systems. Computational imaging is a typical example of this trend, and its application to imaging through strongly scattering media, which are difficult to handle in conventional methods, has been promising. This approach will contribute to various applications, such as life science and industry.

10 Speckle illumination for high- and super-resolution deep imaging (Hilton B. de Aguiar, Sylvain Gigan)

10.1 Status

Microscopy has tremendously advanced in many fronts over the last century. Nowadays, we can image biological specimens at unprecedented time [143], spatial [144], and chemical [145] resolutions. Yet, deep imaging with high resolution in complex media, such as biological tissues, has only recently been tackled actively, and remains a very challenging task. Scattering of light due to inhomogeneities of the medium perturbs the incident illumination and rapidly generates a complex interference pattern: a speckle. Albeit coherent, a speckle presents many features from incoherent illumination. At shallow depth, adaptive optics, mostly borrowing concepts of static objects observed in astronomy, is able to restore a high-quality focus by compensating the low spatial frequency aberrations: these typically arise from weak inhomogeneities of biological tissues. Conversely, wavefront shaping has emerged in the last decade as a powerful tool to directly modify speckles, compensate scattering effects and retrieve a focus at depths surpassing the realm of adaptive optics [7].

An even more challenging aspect is to reach super-resolution imaging in complex media. While structured illumination microscopy (SIM) has been exploited to increase the resolution and allows for depth sectioning [146, 147], it can only be applied to optically thin media. Furthermore, SIM can only reach a few tens of microns at most after the coverslip in high numerical aperture (NA) imaging settings, as it is very sensitive to aberrations and scattering [148]. While most super-resolution techniques have been demonstrated with fluorescence contrast, vibrational contrast still lacks far-field super-resolution capabilities. Regardless of the contrast mechanism, reaching super-resolution in complex media presents itself as a major bottleneck.

In this brief article, we review random (i.e., speckle) illumination for deep imaging, illustrated by two recent experiments, and discuss the opportunities it opens up for deep imaging, including super-resolution.

10.2 Current and future challenges

A first use for random speckle illumination for deep imaging was reported in [149]. In this example, the goal is not super-resolution, but simply to retrieve a fluorescent object at depth, without resorting to wavefront shaping techniques which are lengthy and require expensive spatial-light modulators. A rotating diffuser allows to generate multiple unknown speckle illuminations that illuminate the object at depth, a camera in epi records the fluorescent patterns from the buried object. While a sum of all patterns would be equivalent to a homogeneous incoherent illumination, accessing the individual fluorescent images from each speckle patterns corresponds to recording the same object, under variable and highly inhomogeneous illuminations. Thanks to this property, a computational algorithm allows to determine the pattern coming from every single diffraction spot of the object, and later reconstruct it, a feat that would be extremely difficult (and impossible at depth) using a coherent focused illumination or a completely incoherent one.

A second approach using speckle illumination that we highlight is for super-resolution at moderate depths. In general, there are two large classes of super-resolution approaches: direct and computational. In direct methods, current paradigms are based stimulated emission depletion microscopy (STED) [150], which may image within complex structures; however the resolution limits are sensitive to aberrations that come with complex media. Adaptive optics has been used for STED-like microscopy; however, the depth is still limited to typically one scattering mean free path [151]. Computational approaches are mostly based on the concept of SIM. In SIM, multiple images taken with structured excitation patterns allow access to a larger spatial frequency spectrum of the specimen, beyond the fundamental limits set by the microscope objective NA [148, 151]. The multiple images are then processed with efficient algorithms to reconstruct a super-resolved image. Computational methods typically require wide-field imaging geometries: hence, they are not compatible with thick tissue imaging. This is not particularly a problem for specimens in cell biology (i.e., optically clear samples), where the background is weak, but poses a serious problem for extended tissues as the whole volume generates a strong background that deteriorates the reconstruction quality. As structure patterns, one may use ones with a priori knowledge [146–148, 152], therefore very sensitive to aberrations, or unknown, e.g., speckles, with statistical properties that are resilient to aberrations [153–155]. Yet, using speckles at depth for SIM still remained a challenge for very thick specimens.

The above-mentioned issues are general and others further complicate imaging with vibrational contrast. Many groups are currently searching for new ways to break the diffraction-limit resolution in nonlinear vibrational imaging by far-field methods [156–163], yet the main challenge is to reach universal compatibility with biological specimens. A remarkable achievement has been very recently put forward [162] using STED-like methods. Alternatively, computational methods may allow for all-vibrational-modes super-resolution, in opposition to STED-like methods, and a few demonstrations on SIM combined with Raman scattering have been put forward [164–166], but still suffer from the "thick tissue" issue.

Our recent approach [167] has overcome the fundamental resolution limit in far-field stimulated Raman scattering (SRS) microscopy exploiting SIM with speckle patterns [153, 154]. A particular technological bottleneck for implementing SIM approaches for SRS microscopy is the lack of "cameras" for fast SRS signals readout. Briefly, we developed a solution based on a single-pixel methodology (Fig. 18) that allowed for imaging with depth sectioning capabilities. In the scheme, a (Stokes) beam I_{ro} scanned over a static speckle pattern (pump) beam I_{SI} (ro stands for readout and SI for structured illumination). This scanning scheme, coupled with well-established algorithms [153, 154], was able to recover a super-resolved image. Remarkably, this methodology had a simple microscope alignment procedure providing a series of advantages over conventional SRS and other three-beam super-resolution schemes [156, 162]: it only requires simple superposition of focused beam with a speckle pattern with microscopic precision. Furthermore, the method is applicable to thick tissue imaging due to its quasi-confocal nature thanks to the nonlinear optical process itself. The method overcome the theoretical super-resolution gain for the SRS process by at least a $\sqrt{2}$ in comparison with conventional SRS microscopy with excitation energy densities considerably lower than conventional SRS microscopy.

10.3 Concluding remarks

These two recent experiments highlight many appealing features of speckle patterns for illumination in microscopy: simplicity of generation, resilience to experimental imperfection of the optical system, resilience to scattering and aberrations alike. They provide an unknown but well-controlled illumination, intermediary between scanning and widefield illumination, with diffraction-limited features that in turn unlock many interesting possibilities in imaging, from computational reconstruction to super-resolution.

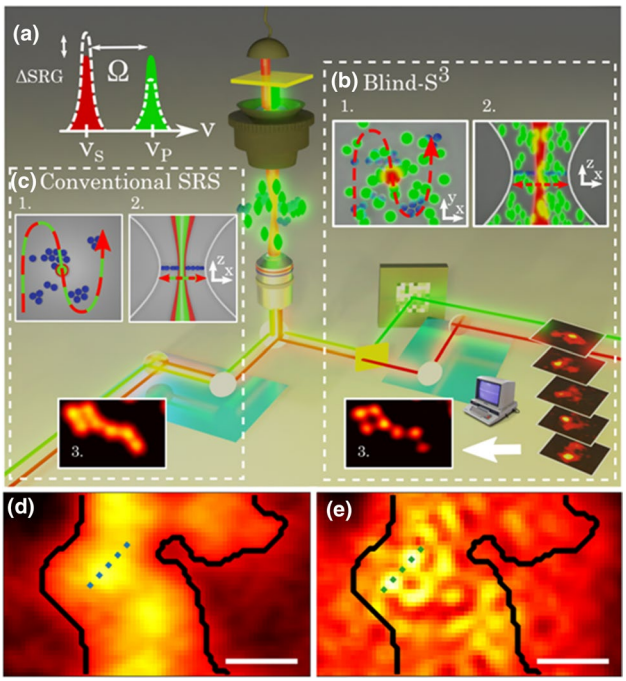

Fig. 18 Principle of speckle-assisted super-resolution SRS. Schematic of the setup to achieve super-resolution using SRS process **a** based on a single-pixel SIM scheme using speckle patterns. View planes of transverse (**b1**) and longitudinal (**b2**) sections containing the Stokes beam (red dash) scanning trajectory over the stationary Raman-active molecules (blue) and structured pump (green). A stack of SRS images from each speckle realization is passed to a SIM algorithm to reconstruct a super-resolved image (**b3**). **c** For comparison, conventional SRS images, consisting in raster scanning co-propagating pump and stokes beams, are taken as a control. View planes of transverse (**c1**) and longitudinal (**c2**) sections of the focused stokes and pump (green and red dash) scanning trajectory over the stationary Raman-active molecules (blue). Conventional (**d**) and super-resolved (**e**) SRS images of 239 nm-diameter polystyrene beads showing the increase in transverse resolution using speckle-assisted SIM. All scale bars: 500 nm

Speckles are not limited to monochromatic lasers as tissues have been shown to disperse spectrally relatively little in the forward scattering regime, therefore only marginally affecting efficiency in nonlinear processes [168–171]. While the examples given here relate to fluorescence and SRS, speckle illumination can also be applied to multiphoton fluorescence imaging, second or third harmonic generation, and coherent and incoherent Raman modalities.

Author contributions All the authors contributed equally to this work. The manuscript was compiled by JR and VA.

Funding Section 2: Israel Science Foundation (1669/16). Section 3: NATO Grant no. SPS-985048 and European Union's Horizon 2020 research and innovation programme under grant agreement No. 857627 (CIPHR). Section 4: this work was supported by the National Natural Science Foundation of China (11534017, 61991450, 61991452, 11704421, 12074444); Department of Education of Guangdong Province (2018KCXTD011); The Key R&D Program of Guangdong Province (2019B010152001); Guangdong Basic and Applied Basic Research Foundation (2020A1515011184); Guangzhou Science and Technology Project (201805010004). Section 5: this work has been funded by the The German Research Association DFG with Grant no. Os 111/49-1 and the Baden-Wuerttemberg Stiftung within the project "Tiefenaufgelöste Fluoreszenzdetektion in streuenden Medien" (FluoTis). We thank our partners at ILM for the production of the phantoms and the collaboration during the project. Mitsuo Takeda is thankful to Alexander von Humboldt Foundation for the opportunity of his research stay at ITO, University of Stuttgart. Section 6: T. Sarkar would like to acknowledge the University Grant Commission, India for financial support as Senior Research Fellowship. Supports from the Science and Engineering Research Board (SERB): CORE/2019/000026 and the Council of Scientific and Industrial Research (CSIR), India-Grant No 80 (0092) /20/EMR-II, are acknowledged. Section 7: this work was supported by KAIST UP program, BK21+ program, Science-X, National Research Foundation of Korea (2015R1A3A2066550, 2021R1C1C2009220), and Institute of Information and communications Technology Planning and Evaluation (IITP) Grant (2021-0-00745). Section 8: this work was supported by the National Natural Science Foundation of China (62061136005, 61991452) and the Key Research Program of Frontier Sciences, Chinese Academy of Sciences (Grant no. QYZDB-SSW-JSC002). Section 10: this research has been funded by the FET-Open (Dynamic-863203), European Research Council ERC Consolidator Grant (SMARTIES-724473).

References

1. G. Satat, M. Tancik, R. Raskar, Towards photography through realistic fog. In Computational Photography (ICCP), 2018 IEEE International Conference on (IEEE, 2018), pp. 1–10
2. S. Narasimhan, S. Nayar, Contrast restoration of weather degraded images. IEEE Trans. Pattern Anal. Mach. Intell. **25**, 713–724 (2003)
3. R. Fattal, Single image dehazing. ACM Trans. Graph (TOG) **27**, 1–9 (2008)
4. R. Horisaki, R. Takagi, J. Tanida, Learning-based imaging through scattering media. Opt. Express **24**, 13738–13743 (2016)
5. K. Lee, Y. Park, Exploiting the speckle-correlation scattering matrix for a compact reference-free holographic image sensor. Nat. Commun. **7**, 13359 (2016)
6. A.K. Singh, D.N. Naik, G. Pedrini, M. Takeda, W. Osten, Exploiting scattering media for exploring 3D objects. Light Sci. Appl. **6**, e16219 (2017)
7. S. Rotter, S. Gigan, Light fields in complex media: mesoscopic scattering meets wave control. Rev. Mod. Phys. **89**, 015005 (2017)
8. A. Vijayakumar, J. Rosen, Interferenceless coded aperture correlation holography—a new technique for recording incoherent digital holograms without two-wave interference. Opt. Express **25**, 13883–13896 (2017)
9. H. Zhuang, H. He, X. Xie, J. Zhou, High speed color imaging through scattering media with a large field of view. Sci. Rep. **6**, 32696 (2016)
10. H. Wang, M. Lyu, G. Situ, eHoloNet: a learning-based end-to-end approach for in-line digital holographic reconstruction. Opt. Express **26**, 22603–22614 (2018)
11. R.K. Singh, Hybrid correlation holography with a single pixel detector. Opt. Lett. **42**, 2515–2518 (2017)

12. V. Anand, S.H. Ng, J. Maksimovic, D. Linklater, T. Katkus, E.P. Ivanova, S. Juodkazis, Single shot multispectral multidimensional imaging using chaotic waves. Sci. Rep. **10**, 13902 (2020)
13. N. Antipa, G. Kuo, R. Heckel, B. Mildenhall, E. Bostan, R. Ng, L. Waller, DiffuserCam: lensless single-exposure 3D imaging. Optica **5**, 1–9 (2018)
14. S.K. Sahoo, D. Tang, C. Dang, Single-shot multispectral imaging with a monochromatic camera. Optica **4**, 1209–1213 (2017)
15. A. Wagadarikar, R. John, R. Willett, D. Brady, Single disperser design for coded aperture snapshot spectral imaging. Appl. Opt. **47**, B44–B51 (2008)
16. J. Bertolotti, E.G. van Putten, C. Blum, A. Lagendijk, W.L. Vos, A.P. Mosk, Non-invasive imaging through opaque scattering layers. Nature **491**, 232–234 (2012)
17. O. Katz, P. Heidmann, M. Fink, S. Gigan, Non-invasive single-shot imaging through scattering layers and around corners via speckle correlations. Nat. Photonics **8**, 784–790 (2014)
18. R. Horisaki, Y. Okamoto, J. Tanida, Single-shot noninvasive three-dimensional imaging through scattering media. Opt. Lett. **44**, 4032–4035 (2019)
19. R.H. Dicke, Scatter-hole cameras for X-rays and gamma rays. Astrophys. J. **153**, L101–L106 (1968)
20. J.R. Fienup, Phase retrieval algorithms: a comparison. Appl. Opt. **21**, 2758–2769 (1982)
21. M.R. Rai, A. Vijayakumar, J. Rosen, Non-linear adaptive three-dimensional imaging with interferenceless coded aperture correlation holography (I-COACH). Opt. Express **26**, 18143–18154 (2018)
22. A.K. Singh, D.N. Naik, G. Pedrini, M. Takeda, W. Osten, Looking through a diffuser and around an opaque surface: a holographic approach. Opt. Express **22**, 7694–7701 (2014)
23. A. Singh, G. Pedrini, M. Takeda, W. Osten, Scatter-plate microscope for lensless microscopy with diffraction limited resolution. Sci. Rep. **7**(1), 10687 (2017)
24. X. Xie, H. Zhuang, H. He, X. Xu, H. Liang, Y. Liu, J. Zhou, Extended depth-resolved imaging through a thin scattering medium with PSF manipulation. Sci. Rep. **8**, 4585 (2018)
25. S.M. Popoff, G. Lerosey, R. Carminati, M. Fink, A.C. Boccara, S. Gigan, Measuring the transmission matrix in optics: an approach to the study and control of light propagation in disordered media. Phys. Rev. Lett. **104**, 100601 (2010)
26. S.M. Popoff, G. Lerosey, M. Fink, A.C. Boccara, S. Gigan, Image transmission through an opaque material. Nat. Commun. **1**, 81 (2010)
27. M. Lyu, H. Wang, G. Li, S. Zheng, G. Situ, Learning-based lensless imaging through optically thick scattering media. Adv. Photonics **1**, 036002 (2019)
28. F. Wang, H. Wang, H. Wang, G. Li, G. Situ, Learning from simulation: an end-to-end deep-learning approach for computational ghost imaging. Opt. Express **27**, 25560–25572 (2019)
29. T. Ando, R. Horisaki, J. Tanida, Speckle-learning-based object recognition through scattering media. Opt. Express **23**, 33902–33910 (2015)
30. A. Vijayakumar, Y. Kashter, R. Kelner, J. Rosen, Coded aperture correlation holography—a new type of incoherent digital holograms. Opt. Express **24**, 12430–12441 (2016)
31. M. Kumar, A. Vijayakumar, J. Rosen, Incoherent digital holograms acquired by interferenceless coded aperture correlation holography system without refractive lenses. Sci. Rep. **7**, 11555 (2017)
32. M.R. Rai, A. Vijayakumar, J. Rosen, Single camera shot interferenceless coded aperture correlation holography. Opt. Lett. **42**, 3992–3995 (2017)
33. M.R. Rai, A. Vijayakumar, J. Rosen, Extending the field of view by a scattering window in an I-COACH system. Opt. Lett. **43**, 1043–1046 (2018)
34. J. Rosen, A. Vijayakumar, M. Kumar, M.R. Rai, R. Kelner, Y. Kashter, A. Bulbul, S. Mukherjee, Recent advances in self-interference incoherent digital holography. Adv. Opt. Photonics **11**, 1–66 (2019)
35. C. Liu, T. Man, Y. Wan, Optimized reconstruction with noise suppression for interferenceless coded aperture correlation holography. Appl. Opt. **59**, 1769–1774 (2020)
36. M.R. Rai, J. Rosen, Noise suppression by controlling the sparsity of the point spread function in interferenceless coded aperture correlation holography (I-COACH). Opt. Express **27**, 24311–24323 (2019)
37. Y. Wan, C. Liu, T. Ma, Y. Qin, S. Lv, Incoherent coded aperture correlation holographic imaging with fast adaptive and noise-suppressed reconstruction. Opt. Express **29**, 8064–8075 (2021)
38. M. Kumar, A. Vijayakumar, J. Rosen, O. Matoba, Interferenceless coded aperture correlation holography with synthetic point spread holograms. Appl. Opt. **59**, 7321–7329 (2020)
39. M.R. Rai, A. Vijayakumar, Y. Ogura, J. Rosen, Resolution enhancement in nonlinear interferenceless COACH with a point response of subdiffraction limit patterns. Opt. Express **27**, 391–403 (2019)
40. M.R. Rai, A. Vijayakumar, J. Rosen, Superresolution beyond the diffraction limit using phase spatial light modulator between incoherently illuminated objects and the entrance of an incoherent imaging system. Opt. Lett. **44**, 1572–1575 (2019)
41. M.R. Rai, J. Rosen, Resolution-enhanced imaging using interferenceless coded aperture correlation holography with sparse point response. Sci. Rep. **10**, 5033 (2020)
42. A. Bulbul, A. Vijayakumar, J. Rosen, Partial aperture imaging by system with annular phase coded masks. Opt. Express **25**, 33315–33329 (2017)
43. N. Dubey, J. Rosen, I. Gannot, High-resolution imaging with annular aperture of coded phase masks for endoscopic applications. Opt. Express **28**, 15122–15137 (2020)
44. A. Bulbul, J. Rosen, Partial aperture imaging system based on sparse point spread holograms and nonlinear cross-correlations. Sci. Rep. **10**, 21983 (2021)
45. N. Hai, J. Rosen, Interferenceless and motionless method for recording digital holograms of coherently illuminated 3-D objects by coded aperture correlation holography system. Opt. Express **27**, 24324–24339 (2019)
46. S. Mukherjee, A. Vijayakumar, J. Rosen, Spatial light modulator aided noninvasive imaging through scattering layers. Sci. Rep. **9**, 17670 (2019)
47. M.R. Rai, J. Rosen, Depth-of-field engineering in coded aperture imaging. Opt. Express **29**, 1634–1648 (2021)
48. V. Anand, S.H. Ng, T. Katkus, S. Juodkazis, White light three-dimensional imaging using a quasi-random lens. Opt. Express **29**(10), 15551–15563 (2021)
49. A. Bulbul, A. Vijayakumar, J. Rosen, Superresolution far-field imaging by coded phase reflectors distributed only along the boundary of synthetic apertures. Optica **5**, 1607–1616 (2018)
50. A. Bulbul, J. Rosen, Super-resolution imaging by optical incoherent synthetic aperture with one channel at a time. Photonics Res. **9**, 1172–1181 (2021)
51. A. Vijayakumar, J. Rosen, Spectrum and space resolved 4D imaging by coded aperture correlation holography (COACH) with diffractive objective lens. Opt. Lett. **42**, 947–950 (2017)
52. A. Vijayakumar, S.H. Ng, T. Katkus, S. Juodkazis, Spatio-spectral-temporal imaging of fast transient phenomena using a random array of pinholes. Adv. Photonics Res. **2**, 2000032 (2021)
53. K.M. Yoo, R.R. Alfano, Time-resolved coherent and incoherent components of forward light scattering in random media. Opt. Lett. **15**, 320–322 (1990)

54. A. Mosk, Y. Silberberg, K. Webb, C. Yang, Imaging, sensing, and communication through highly scattering complex media. Technical report, Defense Technical Information Center (2015)
55. X. Xie, Q. He, Y. Liu, H. Liang, J.Y. Zhou, Non-invasive optical imaging using the extension of the Fourier–domain shower–curtain effect. Opt. Lett. **46**, 98–101 (2021)
56. B.Z. Bentz, B.J. Redman, J.D. van der Laan, K. Westlake, A. Glen, A.L. Sanchez, J.B. Wright, Light transport with weak angular dependence in fog. Opt. Express **29**, 13231–13245 (2021)
57. C. Wu, J.J. Liu, X. Huang, Z.P. Li, C. Yu, J.T. Ye, J. Zhang, Q. Zhang, X.K. Dou, V.K. Goyal, F.H. Xu, J.W. Pan, Non–line-of-sight imaging over 1.43 km. PNAS **118**, e2024468118 (2021)
58. J.W. Goodman, W.H. Huntley Jr., D.W. Jackson, M. Lehmann, Wavefront reconstruction imaging through random media. Appl. Phys. Lett. **8**, 311–313 (1966)
59. J.C. Dainty, D. Newman, Detection of gratings hidden by diffusers using photon-correlation techniques. Opt. Lett. **8**, 608–610 (1983)
60. G. Indebetouw, P. Klysubun, Imaging through scattering media with depth resolution by use of low-coherence gating in spatiotemporal digital holography. Opt. Lett. **25**, 212–214 (2000)
61. Z. Yaqoob, D. Psaltis, M.S. Feld, C. Yang, Optical phase conjugation for turbidity suppression in biological samples. Nat. Photonics **2**, 110–115 (2008)
62. A. Velten, T. Willwacher, O. Gupta, A. Veeraraghavan, M. Bawendi, R. Raskar, Recovering three-dimensional shape around a corner using ultra-fast time-of-flight imaging. Nat. Commun. **3**, 745 (2012)
63. A.P. Mosk, A. Lagendijk, G. Lerosey, M. Fink, Controlling waves in space and time for imaging and focusing in complex media. Nat Photonics **6**, 283–292 (2012)
64. I.M. Vellekoop, A.P. Mosk, Focusing coherent light through opaque strongly scattering media. Opt. Lett. **32**, 2309–2311 (2007)
65. J. Park, J.H. Park, H. Yu, Y.K. Park, Focusing through turbid media by polarization modulation. Opt. Lett. **40**, 1667–1670 (2015)
66. P. Berto, H. Rigneault, M. Guillon, Wavefront sensing with a thin diffuser. Opt. Lett. **24**, 5117–5120 (2017)
67. S. Ludwig, G. Pedrini, X. Peng, W. Osten, Single-pixel scatterplate microscopy. Opt. Lett. **46**, 2473–2476 (2021)
68. J. Schindler, P. Schau, N. Brodhag, K. Frenner, W. Osten, Retrieving the axial position of fluorescent light emitting spots by shearing interferometry. J. Biomed. Opt. **21**, 125009 (2016)
69. D. Huang, E.A. Swanson, C.P. Lin, J.S. Schuman, W.G. Stinson et al., Optical coherence tomography. Science **254**, 1178–1181 (1991)
70. D.N. Naik, R.K. Singh, T. Ezawa, Y. Miyamoto, M. Takeda, Photon correlation holography. Opt. Express **19**, 1408–1421 (2011)
71. M. Takeda, A.K. Singh, D.N. Naik, G. Pedrini, W. Osten, Holographic correloscopy—unconventional holographic techniques for imaging a three-dimensional object through an opaque diffuser or via a scattering wall: a review. IEEE Trans. Ind. Inf. **12**, 1631–1640 (2016)
72. I. Freund, Looking through walls and around corners. Physica A **168**, 49–65 (1990)
73. I. Freund, M. Rosenbluh, S.C. Feng, Memory effects in propagation of optical waves through disordered media. Phys Rev Lett. **61**, 2328–2331 (1988)
74. J.W. Goodman, Analogy between holography and interferometric image formation. J. Opt. Soc. Am. **60**, 506–509 (1970)
75. C. Balch et al., Final version of the American Joint Committee on Cancer staging system for cutaneous melanoma. J. Clin. Oncol. **19**, 3635–3648 (2001)
76. J. Schindler et al., Resolving the depth of fluorescent light by structured illumination and shearing interferometry. Proc. SPIE **9718**, 97182H (2016)
77. W. Osten, K. Frenner, G. Pedrini, A.K. Singh, J. Schindler, M. Takeda, Shaping the light for the investigation of depth-extended scattering media. In *Proceedings of SPIE 10503, Quantitative Phase Imaging IV* (2018), p. 1050318
78. J.T. Sheridan et al., Roadmap on holography. J. Opt. **22**, 123002 (2020)
79. D. Gabor, A new microscopic principle. Nature **161**, 777 (1948). (**(Proc. Roy. Soc. (London) A197, 454 (1949)**))
80. E.N. Leith, J. Upatnieks, Reconstructed wavefronts and communication theory. J. Opt. Soc. Am. **52**, 1123–1130 (1962)
81. I. Yamaguchi, T. Zhang, Phase-shifting digital holography. Opt. Lett. **22**, 1268–1270 (1997)
82. U. Schnars, W. Jüptner, *Digital Holography: Digital Hologram Recording, Numerical Reconstruction and Related Techniques* (Springer, Berlin, 2005)
83. V. Micó, J. García, Z. Zalevsky, Quantitative phase imaging by common-path interferometric microscopy: application to super-resolved imaging and nanophotonics. J. Nanophotonics **3**, 031780 (2009)
84. A. Anand, V. Chhaniwal, B. Javidi, Tutorial: common path self-referencing digital holographic microscopy. Appl. Photonics Lett. **3**, 071101 (2018)
85. M. Takeda, W. Wang, Z. Duan, Y. Miyamoto, Coherence holography. Opt. Express **13**, 9629–9635 (2005)
86. J. Rosen, G. Brooker, Digital spatially incoherent Fresnel holography. Opt. Lett. **32**, 912–914 (2007)
87. L. Mandel, E. Wolf, *Optical Coherence and Quantum Optics* (Cambridge University Press, Cambridge, 2013)
88. R.K. Tyson, *Principle of Adaptive Optics* (CRC Press, Boca Raton, 2019)
89. K.R. Lee, J. Lee, J.-H. Park, J.-H. Park, Y.K. Park, One-wave optical phase conjugation mirror by actively coupling arbitrary light fields into a single-mode reflector. Phys. Rev. Lett. **115**, 153902 (2015)
90. B. Das, N.S. Bisht, R.V. Vinu, R.K. Singh, Lensless complex amplitude image retrieval through a visually opaque scattering medium. Appl. Opt. **56**, 4591–4597 (2017)
91. R.V. Vinu, Z. Chen, J. Pu, Y. Otani, R.K. Singh, Speckle-field digital polarization holographic microscopy. Opt. Lett. **44**, 5711–5714 (2019)
92. B.I. Erkmen, J.H. Shapiro, Ghost imaging: from quantum to classical to computational. Adv. Opt. Photonics **2**, 405–450 (2010)
93. P. Clemente, V. Durán, E. Tajahuerce, V. Torres-Company, J. Lancis, Single-pixel digital ghost holography. Phys. Rev. A. **86**, 41803 (2012)
94. R.V. Vinu, Z. Chen, R.K. Singh, J. Pu, Ghost diffraction holographic microscopy. Optica **7**, 1697–1704 (2020)
95. A.S. Somkuwar, B. Das, R.V. Vinu, Y.K. Park, R.K. Singh, Holographic imaging through a scattering layer using speckle interferometry. J. Opt. Soc. Am. A **34**, 1392–1399 (2017)
96. J. Goodman, *Statistical Optics* (Wiley, New York, 2000)
97. M. Takeda et al., Spatial statistical optics and spatial correlation holography: a review. Opt. Rev. **21**, 849–861 (2014)
98. D.N. Naik, T. Ezawa, R.K. Singh, Y. Miyamoto, M. Takeda, Coherence holography by achromatic 3-D field correlation of generic thermal light with an imaging Sagnac shearing interferometer. Opt. Express **20**, 19658–19669 (2012)
99. L. Chen, R.K. Singh, Z. Chen, J. Pu, Phase shifting digital holography with the Hanbury Brown–Twiss approach. Opt. Lett. **45**, 212–215 (2020)
100. Y. Park, C. Depeursinge, G. Popescu, Quantitative phase imaging in biomedicine. Nat. Photonics **12**, 578–589 (2002)

101. K. Lee, K. Kim, J. Jung, J. Heo, S. Cho, S. Lee, G. Chang, Y. Jo, H. Park, Y. Park, Quantitative phase imaging techniques for the study of cell pathophysiology: from principles to applications. Sensors **13**, 4170–4191 (2002)
102. G. Popescu, Y. Park, N. Lue, C. Best-Popescu, L. Deflores, R.R. Dasari, M.S. Feld, K. Badizadegan, Optical imaging of cell mass and growth dynamics. Am. J. Physiol. Cell Physiol. **295**, C538–C544 (2008)
103. Y. Park, W. Choi, Z. Yaqoob, R. Dasari, K. Badizadegan, M.S. Feld, Speckle-field digital holographic microscopy. Opt. Express **17**, 12285–12292 (2009)
104. G. Choi, D. Ryu, Y. Jo, Y.S. Kim, W. Park, H.-S. Min, Y. Park, Cycle-consistent deep learning approach to coherent noise reduction in optical diffraction tomography. Opt. Express **27**, 4927–4943 (2019)
105. D. Ryu, Y. Jo, J. Yoo, T. Chang, D. Ahn, Y.S. Kim, G. Kim, H.-S. Min, Y. Park, Deep learning-based optical field screening for robust optical diffraction tomography. Sci. Rep. **9**, 1–9 (2019)
106. Z. Wang, L. Millet, M. Mir, H. Ding, S. Unarunotai, J. Rogers, M.U. Gillette, G. Popescu, Spatial light interference microscopy (SLIM). Opt. Express **19**, 1016–1026 (2011)
107. T.H. Nguyen, M.E. Kandel, M. Rubessa, M.B. Wheeler, G. Popescu, Gradient light interference microscopy for 3D imaging of unlabeled specimens. Nat. Commun. **8**, 1–9 (2017)
108. P. Bon, G. Maucort, B. Wattellier, S. Monneret, Quadriwave lateral shearing interferometry for quantitative phase microscopy of living cells. Opt. Express **17**, 13080–13094 (2009)
109. X. Ou, R. Horstmeyer, C. Yang, G. Zheng, Quantitative phase imaging via Fourier ptychographic microscopy. Opt. Lett. **38**, 4845–4848 (2013)
110. Y. Baek, Y. Park, Intensity-based holographic imaging via space-domain Kramers–Kronig relations. Nat. Photonics **15**, 354–360 (2021)
111. J. Li, A. Matlock, Y. Li, Q. Chen, C. Zuo, L. Tian, High-speed in vitro intensity diffraction tomography. Adv. Photonics **1**, 33 (2019)
112. J.M. Soto, J.A. Rodrigo, T. Alieva, Label-free quantitative 3D tomographic imaging for partially coherent light microscopy. Opt. Express **25**, 15699–15712 (2017)
113. R. Ling, W. Tahir, H.-Y. Lin, H. Lee, L. Tian, High-throughput intensity diffraction tomography with a computational microscope. Biomed. Opt. Express **9**, 2130–2141 (2018)
114. A. Matlock, L. Tian, High-throughput, volumetric quantitative phase imaging with multiplexed intensity diffraction tomography. Biomed. Opt. Express **10**, 6432–6448 (2019)
115. H. Hugonnet, M. Lee, Y. Park, Optimizing illumination in three-dimensional deconvolution microscopy for accurate refractive index tomography. Opt. Express **29**, 6293–6301 (2021)
116. Y. Baek, K. Lee, J. Oh, Y. Park, Speckle-correlation scattering matrix approaches for imaging and sensing through turbidity. Sensors **20**, 3147 (2020)
117. Y. Baek, K. Lee, Y. Park, High-resolution holographic microscopy exploiting speckle-correlation scattering matrix. Phys. Rev. Appl. **10**, 024053 (2018)
118. K. Lee, Y. Park, Interpreting intensity speckle as the coherency matrix of classical light. Phys. Rev. Appl. **12**, 024003 (2019)
119. I. Godfellow, Y. Bengio, A. Courville, *Deep Learning* (MIT Press, New York, 2016)
120. Y. Rivenson, Y. Zhang, H. Gunaydin, D. Teng, A. Ozcan, Phase recovery and holographic image reconstruction using deep learning in neural networks. Light Sci. Appl. **7**, 17141 (2018)
121. J. Li, D. Wang, S. Li, M. Zhang, C. Song, X. Chen, Deep learning based adaptive sequential data augmentation technique for the optical network traffic synthesis. Opt. Express **27**, 18831–18847 (2019)
122. F. Wang, Y. Bian, H. Wang, M. Lyu, G. Pedrini, W. Osten, G. Barbastathis, G. Situ, "Phase imaging with an untrained neural network. Light Sci. Appl. **9**, 77 (2020)
123. A. Sinha, J. Lee, S. Li, G. Barbastathis, Lensless computational imaging through deep learning. Optica **4**, 1117–1125 (2017)
124. Y. Li, Y. Xue, L. Tian, Deep speckle correlation: a deep learning approach toward scalable imaging through scattering media. Optica **5**, 1181–1190 (2018)
125. S. Zheng, H. Wang, S. Dong, F. Wang, G. Situ, Incoherent imaging through highly nonstatic and optically thick turbid media based on neural network. Photonics Res. **9**, B220–B228 (2021)
126. S. Zhu, E. Guo, J. Gu, L. Bai, J. Han, Imaging through unknown scattering media based on physics-informed learning. Photonics Res. **9**, B210–B219 (2021)
127. K. Johnstonbaugh, S. Agrawal, D.A. Durairaj, C. Fadden, A. Dangi, S.P.K. Karri, S.-R. Kothapalli, A deep learning approach to photoacoustic wavefront localization in deep-tissue medium. IEEE Trans. Ultrason. Ferroelectr. Freq. Control **67**, 2649–2659 (2020)
128. A. Matlock, L. Tian, in *Physical Model Simulator-Trained Neural Network for Computational 3D Phase Imaging of Multiple-Scattering Samples*. arXiv:2103.15795 (2021)
129. R. Horstmeyer, H. Ruan, C. Yang, Guidestar-assisted wavefront-shaping methods for focusing light into biological tissue. Nat. Photonics **9**, 563–571 (2015)
130. R.G. Baraniuk, Compressive sensing [lecture notes]. IEEE Signal Process. Mag. **24**, 118–121 (2007)
131. Y. LeCun, Y. Bengio, G. Hinton, Deep learning. Nature **521**, 436–444 (2015)
132. Y. Okamoto, R. Horisaki, J. Tanida, Noninvasive three-dimensional imaging through scattering media by three-dimensional speckle correlation. Opt. Lett. **44**, 2526–2529 (2019)
133. X. Xu, X. Xie, H. He, H. Zhuang, J. Zhou, A. Thendiyammal, A.P. Mosk, Imaging objects through scattering layers and around corners by retrieval of the scattered point spread function. Opt. Express **25**, 32829–32840 (2017)
134. K. Ehira, R. Horisaki, Y. Nishizaki, M. Naruse, J. Tanida, Spectral speckle-correlation imaging. Appl. Opt. **60**, 2388–2392 (2021)
135. G. Barbastathis, A. Ozcan, G. Situ, On the use of deep learning for computational imaging. Optica **6**, 921–943 (2019)
136. R. Takagi, R. Horisaki, J. Tanida, Object recognition through a multi-mode fiber. Opt. Rev. **24**, 117–120 (2017)
137. R. Horisaki, F. Kazuki, J. Tanida, Single-shot and lensless complex-amplitude imaging with incoherent light based on machine learning. Opt. Rev. **25**, 593–597 (2018)
138. R. Horisaki, R. Takagi, J. Tanida, Learning-based focusing through scattering media. Appl. Opt. **56**, 4358–4362 (2017)
139. R. Horisaki, Y. Mori, J. Tanida, Incoherent light control through scattering media based on machine learning and its application to multiview stereo displays. Opt. Rev. **26**, 709–712 (2019)
140. R. Horisaki, R. Takagi, J. Tanida, Learning-based single-shot superresolution in diffractive imaging. Appl. Opt. **56**, 8896–8901 (2017)
141. R. Horisaki, R. Takagi, J. Tanida, Deep-learning-generated holography. Appl. Opt. **57**, 3859–3863 (2018)
142. R. Horisaki, Y. Nishizaki, K. Kitaguchi, M. Saito, J. Tanida, Three-dimensional deeply generated holography [Invited]. Appl. Opt. **60**, A323–A328 (2021)
143. L. Gao, J. Liang, C. Li, L.V. Wang, Single-shot compressed ultrafast photography at one hundred billion frames per second. Nature **516**, 74–77 (2014)
144. F. Balzarotti, Y. Eilers, K.C. Gwosch, A.H. Gynnå, V. Westphal, F.D. Stefani, J. Elf, S.W. Hell, Nanometer resolution imaging and

tracking of fluorescent molecules with minimal photon fluxes. Science **355**, 606–612 (2017)
145. B.G. Saar, C.W. Freudiger, J. Reichman, C.M. Stanley, G.R. Holtom, X.S. Xie, Video-rate molecular imaging in vivo with stimulated Raman scattering. Science **330**, 1368–1370 (2010)
146. M.G.L. Gustafsson, Surpassing the lateral resolution limit by a factor of two using structured illumination microscopy. J. Microsc. **198**, 82–87 (2000)
147. R. Heintzmann, C.G. Cremer, Laterally modulated excitation microscopy: improvement of resolution by using a diffraction grating, in *Optical Biopsies and Microscopic Techniques III*, vol. 3568, ed. by I.J. Bigio, H. Schneckenburger, J. Slavik, K. Svanberg, P.M. Viallet (Stockholm, Sweden, SPIE, 1999), pp. 185–196.
148. Y. Wu, H. Shroff, Faster, sharper, and deeper: structured illumination microscopy for biological imaging. Nat. Methods **15**(12), 1011–1019 (2018)
149. L. Zhu, F. Soldevila, C. Moretti, A. d'Arco, A. Boniface, X. Shao, H.B. de Aguiar, S. Gigan, Large field-of-view non-invasive imaging through scattering layers using fluctuating random illumination (2021). arXiv:2107.08158
150. S.W. Hell, J. Wichmann, Breaking the diffraction resolution limit by stimulated emission: stimulated-emission-depletion fluorescence microscopy. Opt. Lett. **19**, 780 (1994)
151. X. Hao, E.S. Allgeyer, D.-R. Lee, J. Antonello, K. Watters, J.A. Gerdes, L.K. Schroeder, F. Bottanelli, J. Zhao, P. Kidd, M.D. Lessard, J.E. Rothman, L. Cooley, T. Biederer, M.J. Booth, J. Bewersdorf, Three-dimensional adaptive optical nanoscopy for thick specimen imaging at sub-50-nm resolution. Nat. Methods **18**, 688–693 (2021)
152. F. Ströhl, C.F. Kaminski, Frontiers in structured illumination microscopy. Optica **3**, 667–677 (2016)
153. E. Mudry, K. Belkebir, J. Girard, J. Savatier, E. Le Moal, C. Nicoletti, M. Allain, A. Sentenac, Structured illumination microscopy using unknown speckle patterns. Nat. Photonics **6**, 312–315 (2012)
154. L.-H. Yeh, L. Tian, L. Waller, Structured illumination microscopy with unknown patterns and a statistical prior. Biomed. Opt. Express **8**, 695 (2017)
155. H. Yilmaz, E.G. van Putten, J. Bertolotti, A. Lagendijk, W.L. Vos, A.P. Mosk, Speckle correlation resolution enhancement of wide-field fluorescence imaging. Optica **2**, 424–429 (2015)
156. R.C. Prince, R.R. Frontiera, E.O. Potma, Stimulated raman scattering: from bulk to nano. Chem. Rev. **117**, 5070–5094 (2017)
157. W.R. Silva, C.T. Graefe, R.R. Frontiera, Toward label-free super-resolution microscopy. ACS Photonics **3**, 79–86 (2016)
158. A. Gasecka, A. Daradich, H. Dehez, M. Piché, D. Côté, Resolution and contrast enhancement in coherent anti-Stokes Raman-scattering microscopy. Opt. Lett. **38**, 4510–4513 (2013)
159. Y. Yonemaru, A.F. Palonpon, S. Kawano, N.I. Smith, S. Kawata, K. Fujita, Super-spatial- and -spectral-resolution in vibrational imaging via saturated coherent anti-Stokes Raman scattering. Phys. Rev. Appl. **4**, 14010 (2015)
160. C. Cleff, P. Groß, C. Fallnich, H.L. Offerhaus, J.L. Herek, K. Kruse, W.P. Beeker, C.J. Lee, K.-J. Boller, Ground-state depletion for subdiffraction-limited spatial resolution in coherent anti-Stokes Raman scattering microscopy. Phys. Rev. A **86**, 23825 (2012)
161. H. Kim, G.W. Bryant, S.J. Stranick, Superresolution four-wave mixing microscopy. Opt. Express **20**, 6042–6051 (2012)
162. H. Xiong, N. Qian, Y. Miao, Z. Zhao, C. Chen, W. Min, Super-resolution vibrational microscopy by stimulated Raman excited fluorescence. Light Sci. Appl. **10**, 87 (2021)
163. L. Gong, W. Zheng, Y. Ma, Z. Huang, Saturated stimulated-Raman-scattering microscopy for far-field superresolution vibrational imaging. Phys. Rev. Appl. **11**, 034041 (2019)
164. K.M. Hajek, B. Littleton, D. Turk, T.J. McIntyre, H. Rubinsztein-Dunlop, A method for achieving super-resolved widefield CARS microscopy. Opt. Express **18**, 19263–19272 (2010)
165. K. Watanabe, A.F. Palonpon, N.I. Smith, A. Kasai, H. Hashimoto, S. Kawata, K. Fujita et al., Structured line illumination Raman microscopy. Nat. Commun. **6**, 10095 (2015)
166. J.H. Park, S.-W. Lee, E.S. Lee, J.Y. Lee, A method for super-resolved CARS microscopy with structured illumination in two dimensions. Opt. Express **22**, 9854–9870 (2014)
167. J. Guilbert, A. Negash, S. Labouesse, S. Gigan, A. Sentenac, H.B. de Aguiar, Label-free super-resolution chemical imaging of biomedical specimens. bioRxiv 2021.05.14.444185 (2021)
168. P. Arjmand, O. Katz, S. Gigan, M. Guillon, Three-dimensional broadband light beam manipulation in forward scattering samples. Opt. Express **29**, 6563–6581 (2020)
169. A.G. Vesga, M. Hofer, N.K. Balla, H.B. de Aguiar, M. Guillon, S. Brasselet, Focusing large spectral bandwidths through scattering media. Opt. Express **27**, 28384–28394 (2019)
170. M. Hofer, S. Shivkumar, B. El Waly, S. Brasselet, Coherent anti-stokes raman scattering through thick biological tissues by single-wavefront shaping. Phys. Rev. Appl. **14**, 024019 (2020)
171. H.B. De Aguiar, S. Gigan, S. Brasselet, Enhanced nonlinear imaging through scattering media using transmission-matrix-based wave-front shaping. Phys. Rev. A **94**, 43830 (2016)